Ground-based remote sensing of the atmospheric boundary layer for wind energy site assessment

Stefan Emeis
stefan.emeis@kit.edu

INSTITUTE OF METEOROLOGY AND CLIMATE RESEARCH, Atmospheric Environmental Research

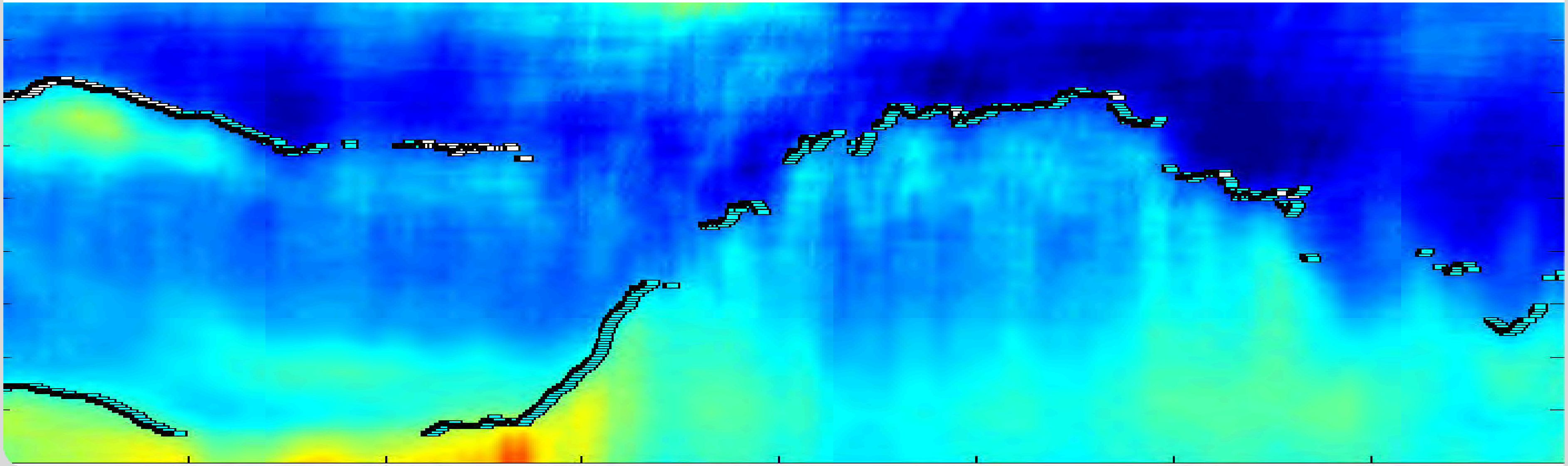

wind energy-related phenomena

Surface/mixing layer height influences diurnal variation of vertical wind profiles

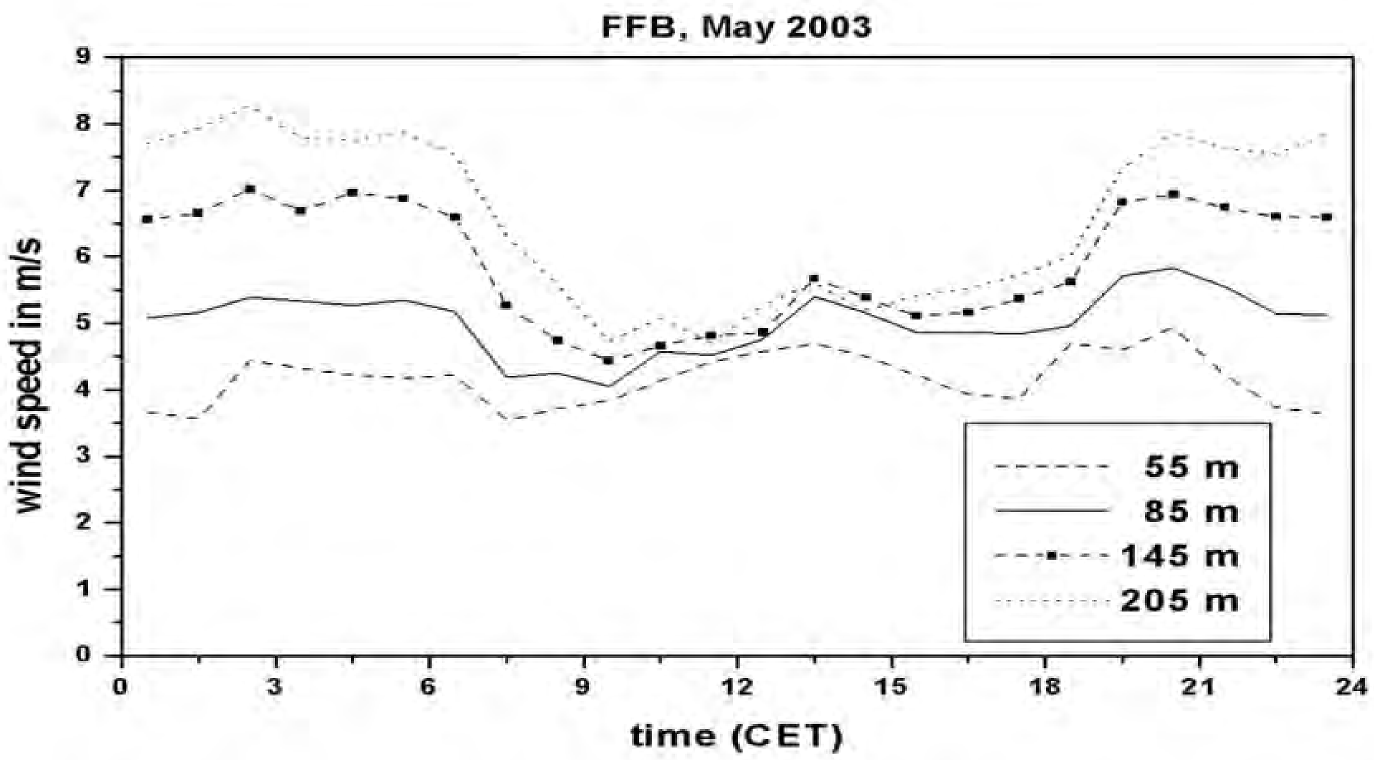

Surface/mixing layer height influences diurnal variation of vertical wind profiles

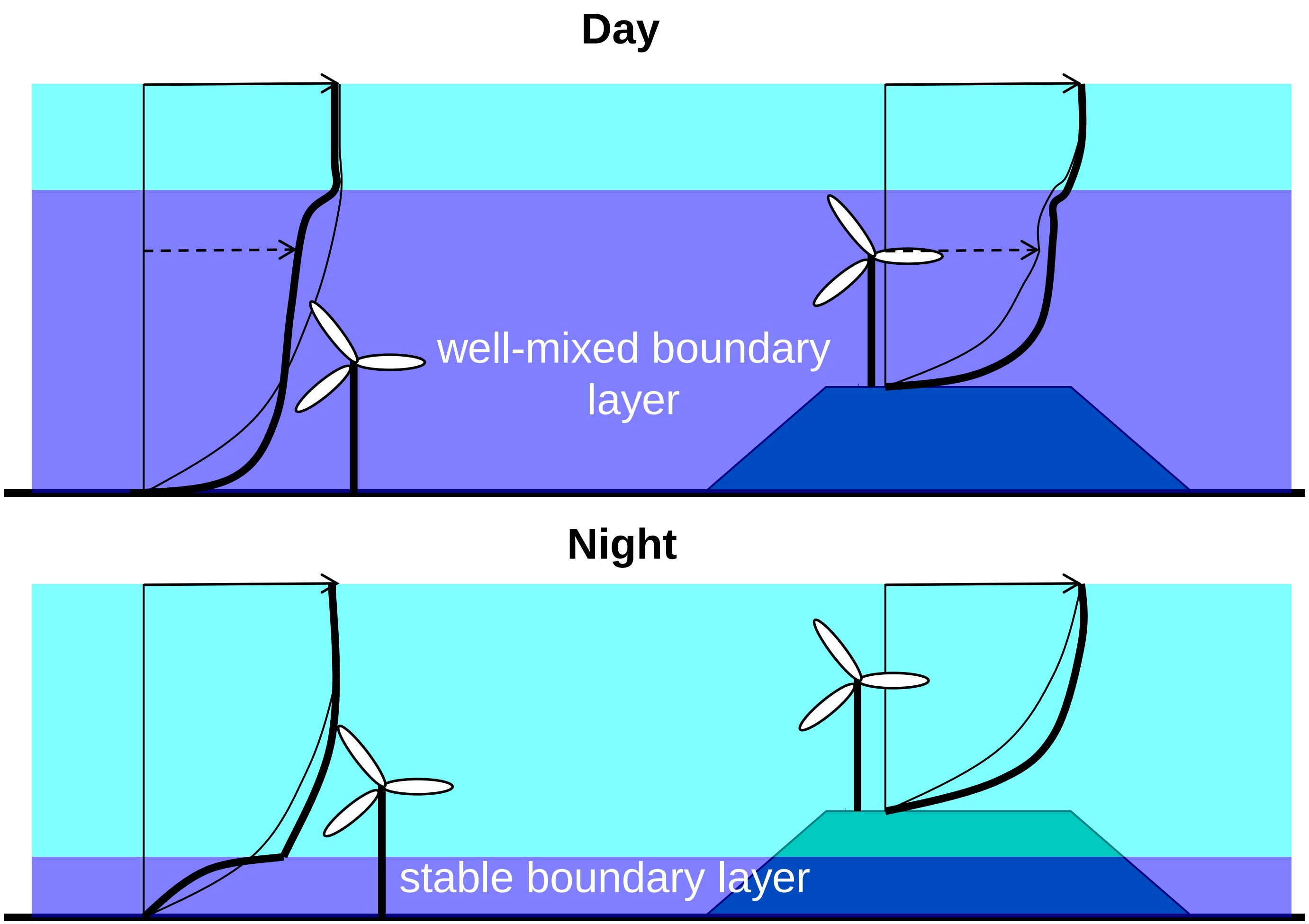

Low-level jet

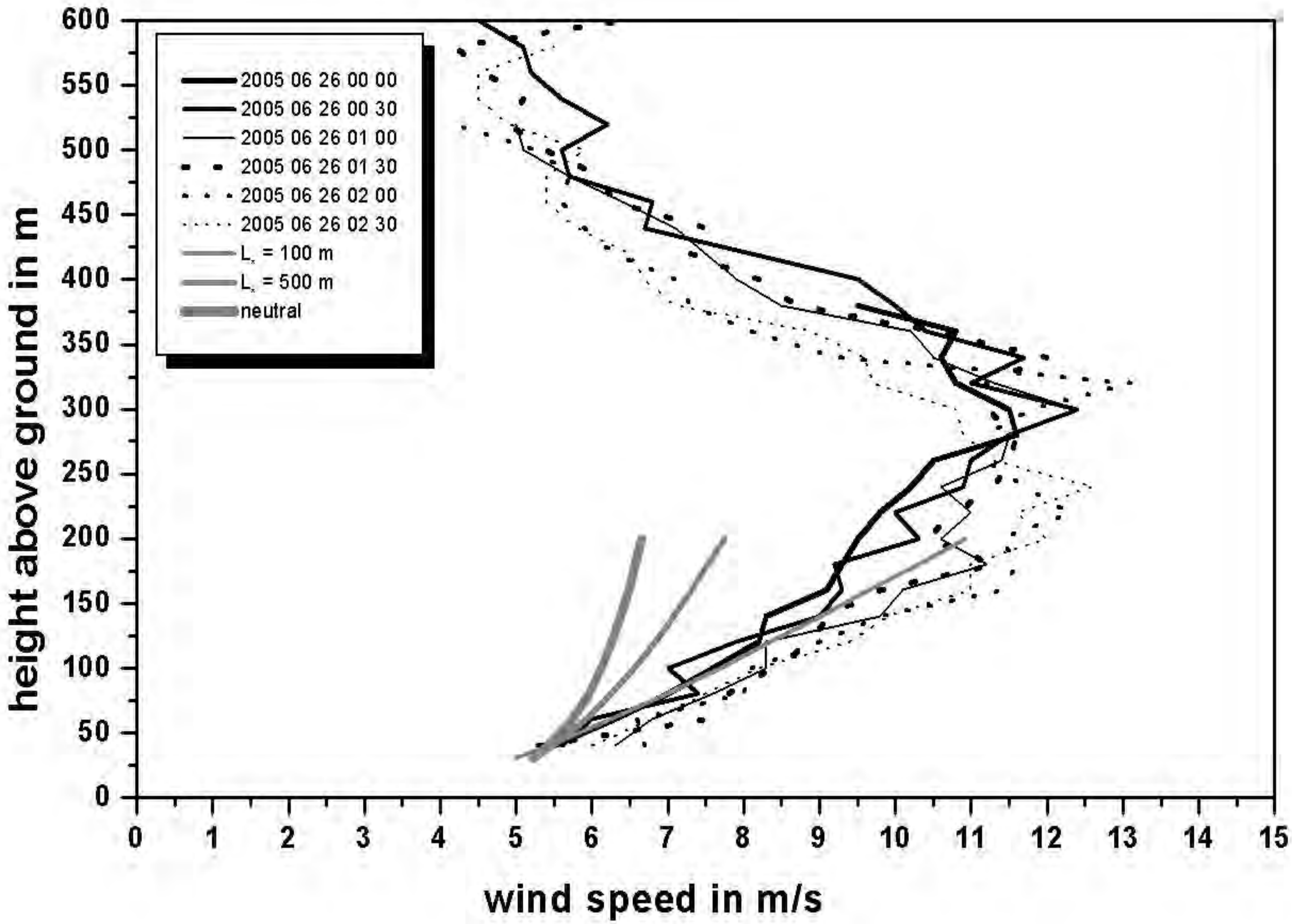

vertical profiles of wind speed

26 June 2005

AdP Ch d G

Nocturnal low-level jet and the turning of wind direction with height

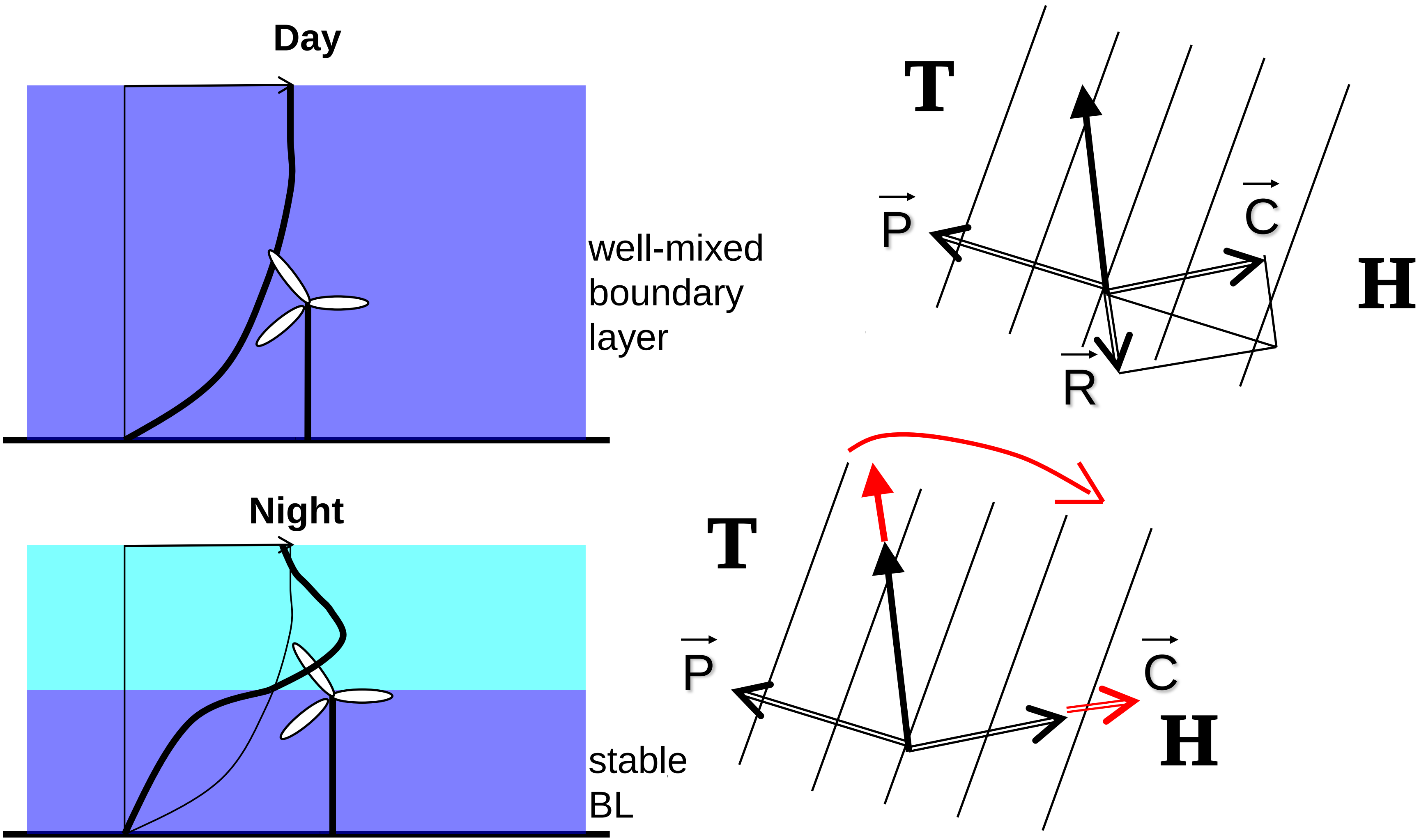

surface pressure
00 GMT

26 June 2005

asterisk denotes location where LLJ was observed

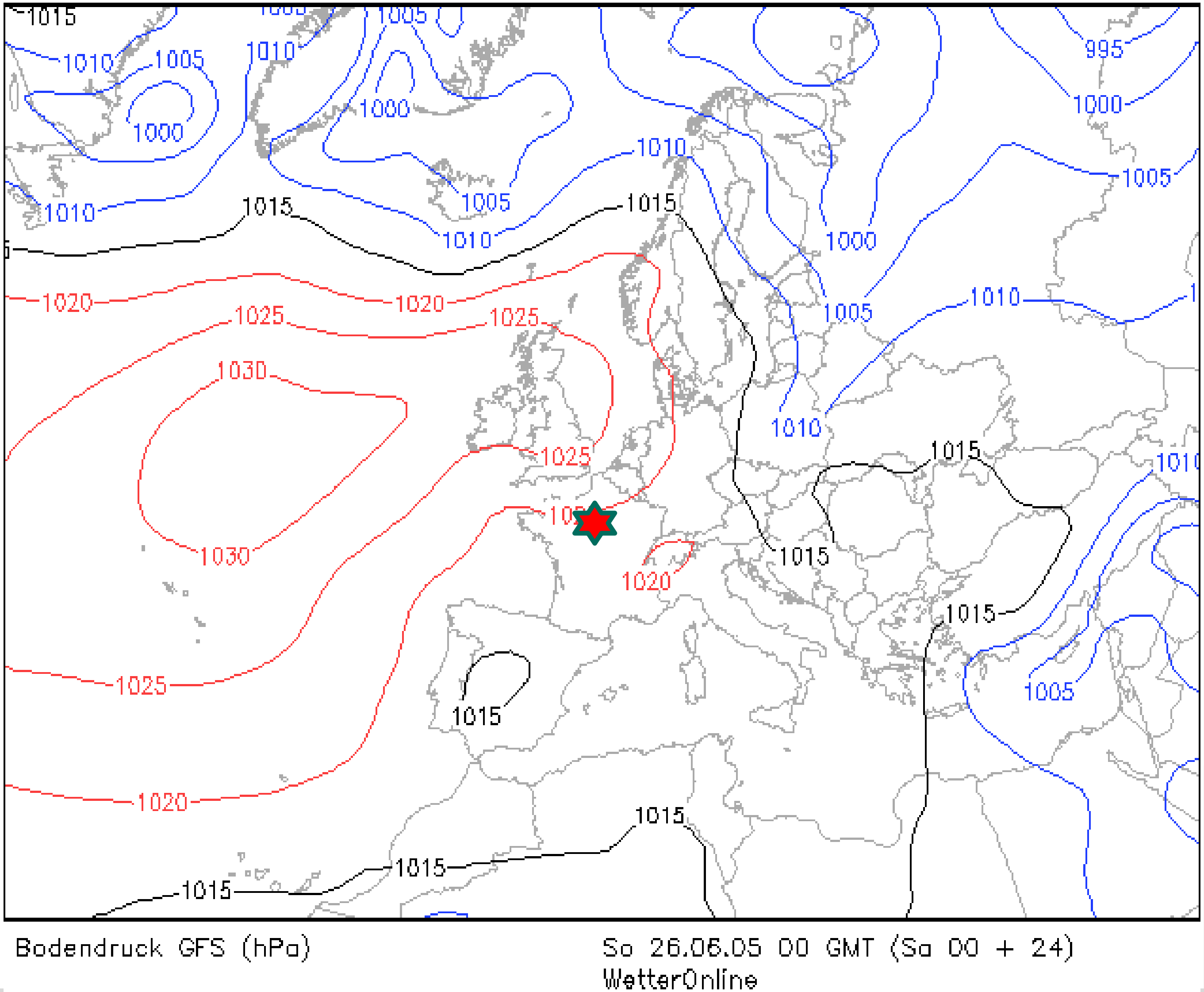

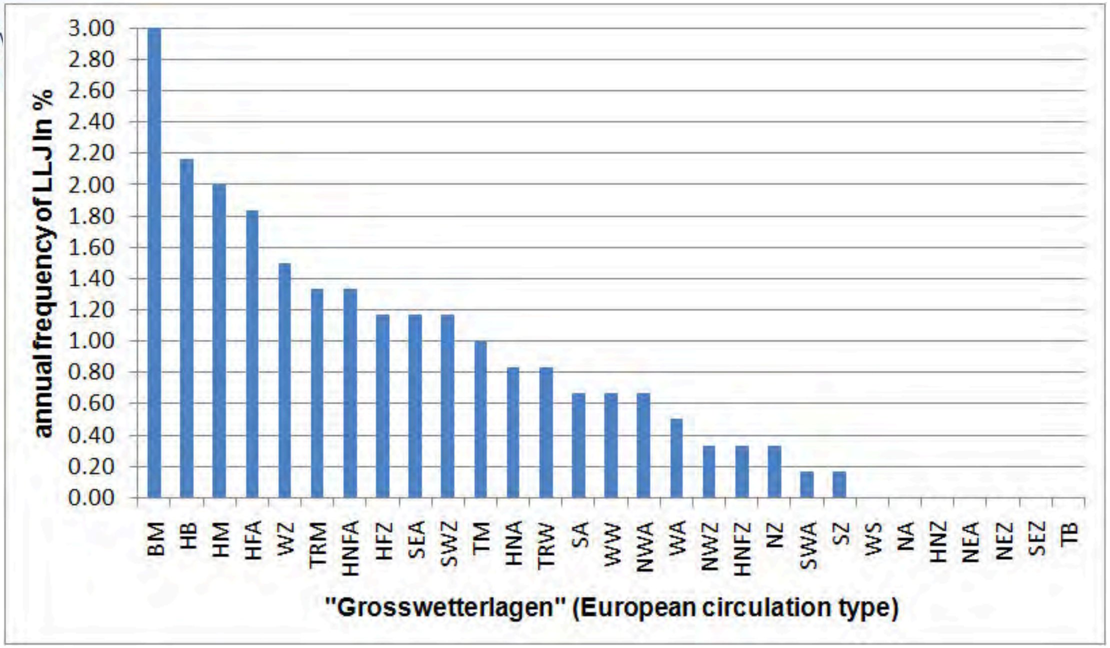

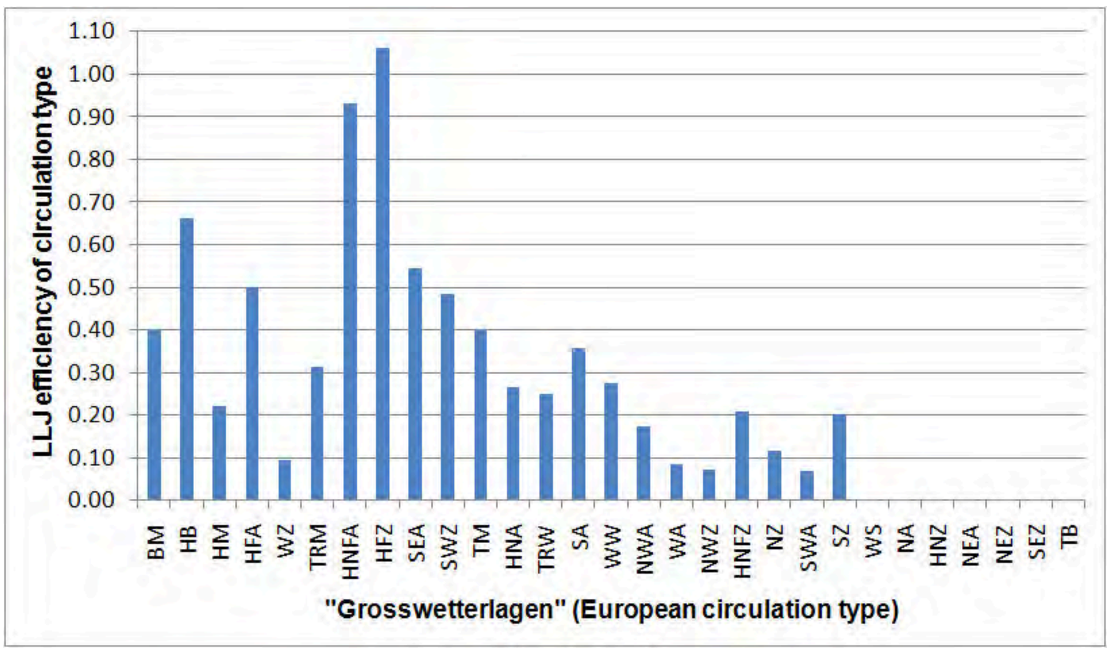

Karlsruhe Institute of Technology

frequency of LLJ over Hanover for 20 months in the years 2001 to 2003

total is 23.17% of all nights

circulation types:

BM ridge over Central Europe
HB high over British Isles
HM high over Central Europe
...

HFZ high over Scandinavia
HNFA high over North Atlantic
...

"efficiency" of a circulation type to produce a LLJ over Hanover for 20 months in the years 2001 to 2003

Relevance for wind energy

The vertical wind profile (equilibrium conditions)

logarithmic law
(with stability correction) $u(z) = (u_*/\kappa)\,(\ln(z/z_0) - \psi(z/L_*))$

power law $u(z) = u(z_A)\,(z/z_A)^n$

New proposal
(Gryning et al. 2007)

$$u(z) = \frac{u_{*0}}{\kappa}\left(\ln\left(\frac{z}{z_0}\right) + \frac{z}{L_{MBL,N}} - \frac{z}{z_i}\left(\frac{z}{2L_{MBL,N}}\right)\right)$$

needs information on the PBL or mixing-layer height

Gryning, S.-E., E. Batchvarova, B. Brümmer, H. Jørgensen, S. Larsen, 2007: On the extension of the wind profile over homogeneous terrain beyond the surface boundary layer. Bound.-Lay. Meteorol., **124**, 251–268.

Peña, A., S.-E. Gryning, C.B. Hasager, 2010: Comparing mixing-length models of the diabatic wind profile over homogeneous terrain. Theor. Appl. Climatol., **100**, 325-353.

LLJ can only be described by time-dependent equations!

WindForS Wind Energy Research Alliance

Basic remote sensing techniques

KIT Karlsruhe Institute of Technology

name	princple	spatial resolution	direction	type
RADAR	backscatter, electro-magnetic pulses, fixed wave length	profiling	scanning, slanted	active, monostatic
SODAR	backscatter, acoustic pulses, fixed wave length	profiling	fixed, slanted, vertical	active, usually monostatic
LIDAR ceilometer	backscatter, optical pulses, fixed wave length(s)	profiling	scanning, fixed, horizontal, slanted, vertical	active, monostatic
RASS	backscatter, acoustic, electro-magnetic, fixed wave length	profiling	fixed, vertical	active, monostatic
FTIR	absorption, infrared, spectrum	path-averaging	fixed, horizontal, slanted	active, bistatic or passive
	emission, infrared, spectrum	path-averaging	fixed, horizontal, slanted	passive
DOAS	absorption, optical, fixed wave lengths	path-averaging	fixed, horizontal	active, bistatic
radiometry	electro-magnetic, fixed wave length(s)	averaging, profiling	fixed, scanning, slanted, vertical	passive
tomography	travel time, acoustic, fixed wave length	horizontal distribution	fixed, horizontal	active, multiple emitters and receivers

subject of this lecture

subject of this lecture

Frequencies for atmospheric remote sensing

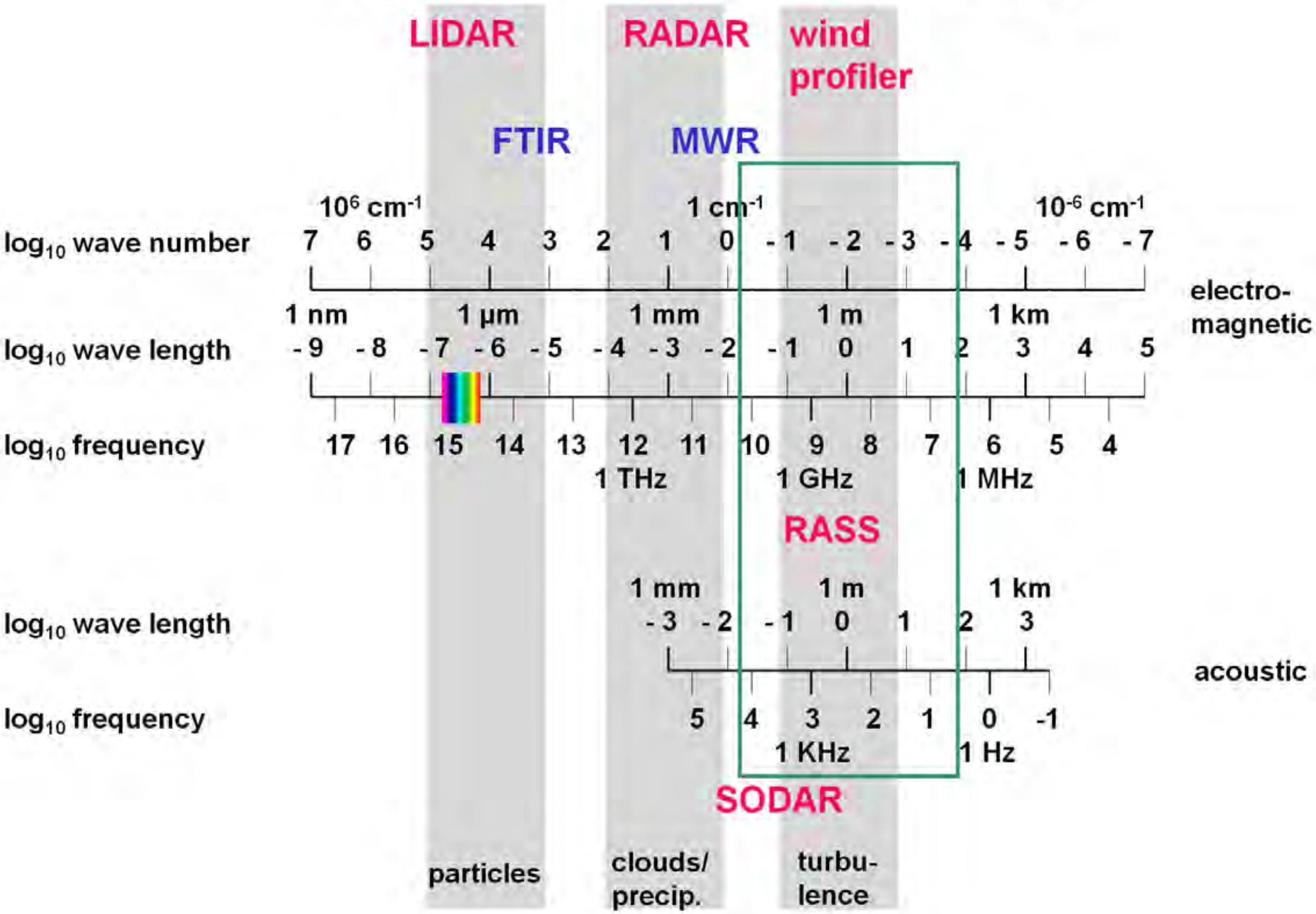

Emeis, S., 2010: Measurement Methods in Atmospheric Sciences - In situ and remote. Borntraeger, Stuttgart, 272 pp., 103 figs, 28 tables, ISBN 978-3-443-01066-9.

Surface-based Remote Sensing Systems

at IMK-IFU

SODAR (Large system), acoustic backscatter, Doppler shift analysis ➔ wind, turbulence

SODAR-RASS (Doppler-RASS), acoustic, electro-magnetic backscatter, determines speed of sound ➔ wind and temperature profiles

Ceilometer, backscatter, optical pulses, wave length ~ 0.9 µm ➔ aerosol profiles

Wind-LIDAR, optical backscatter, Doppler shift analysis, wave length ~ 1.5 µm ➔ wind and aerosol profiles

image: Halo Photonics

SODAR

wind, turbulence, mixing-layer height, low-level jets

stefan.emeis@kit.edu Institute for Meteorology and Climate Research – Atmospheric Environmental Research

monostatic SODAR: measuring principles

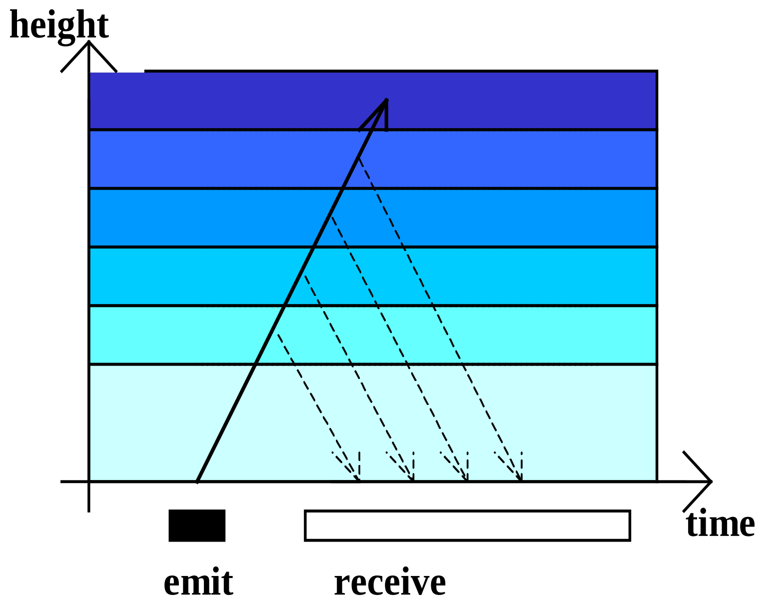

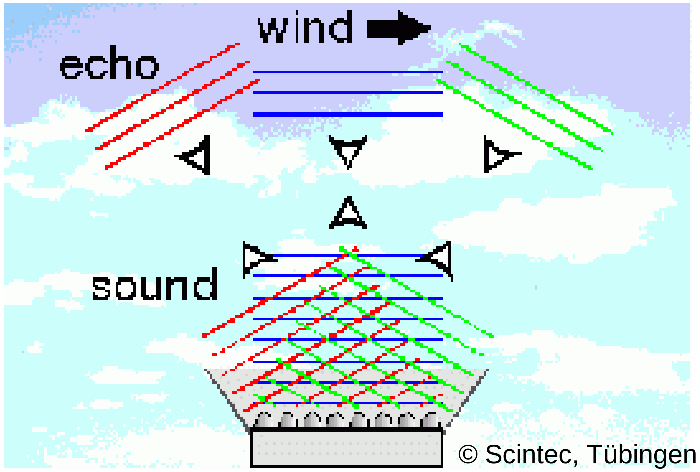

deduction:

sound travel time = height
backscatter intensity = turbulence
Doppler-shift = wind speed

Emission of sound waves into three directions:

in order to measure all three components of the wind (horizontal and vertical)

SODAR sample plot (daytime convective BL)

acoustic backscatter intensity

40 – 300 m

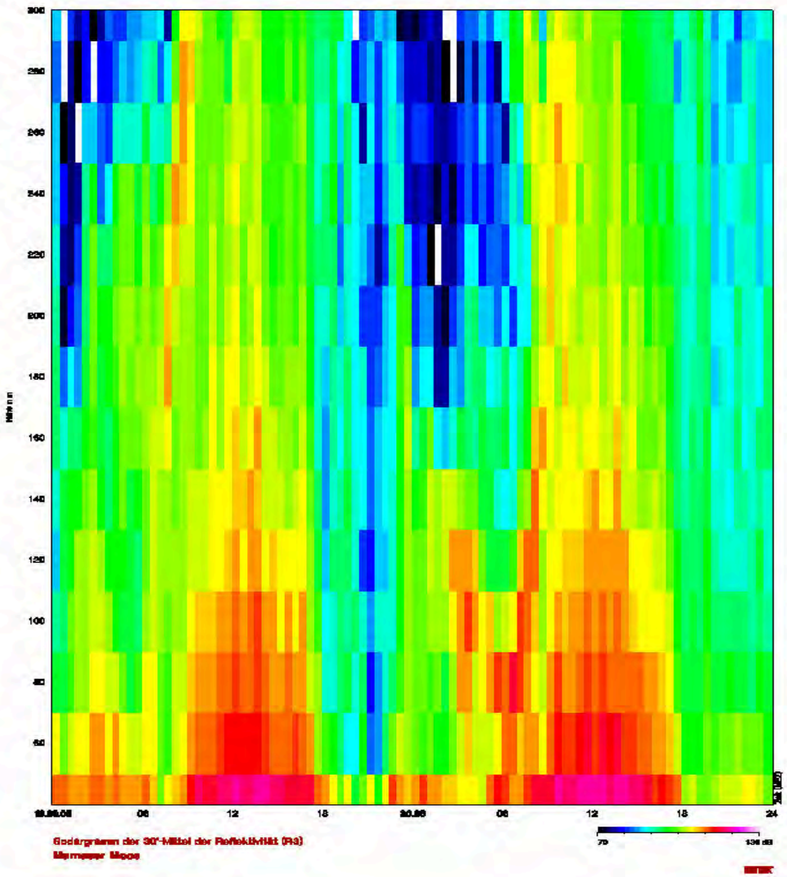

2 days, midnight to midnight

sigma w

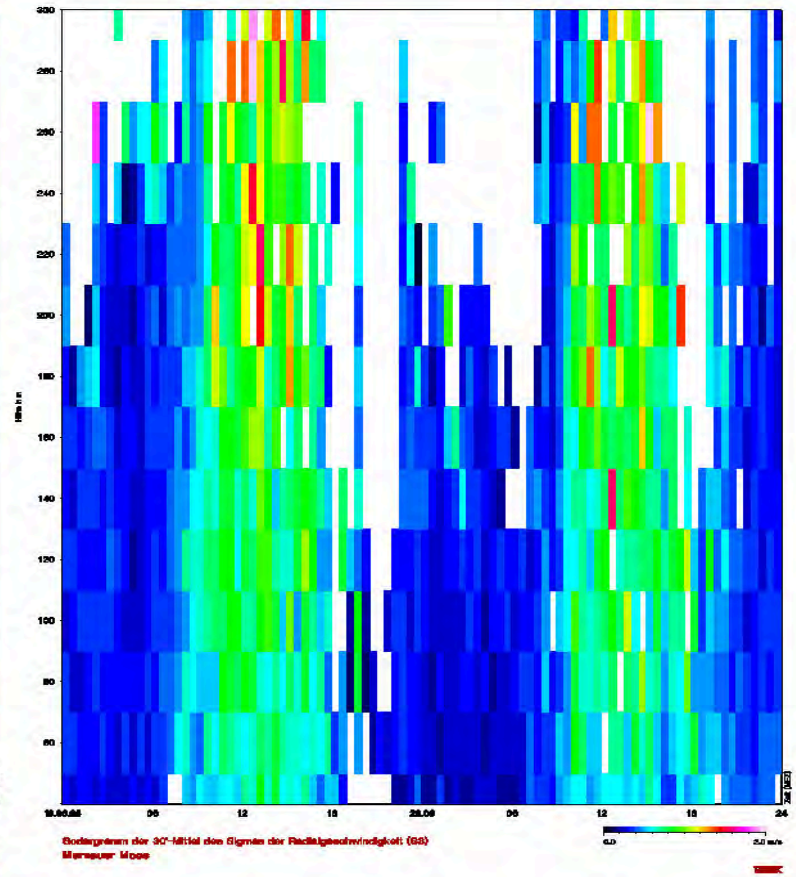

stefan.emeis@kit.edu Institute for Meteorology and Climate Research – Atmospheric Environmental Research

WindForS Wind Energy Research Alliance

Karlsruhe Institute of Technology

SODAR sample plot (lifted inversion)

acoustic backscatter intensity

40 – 400 m

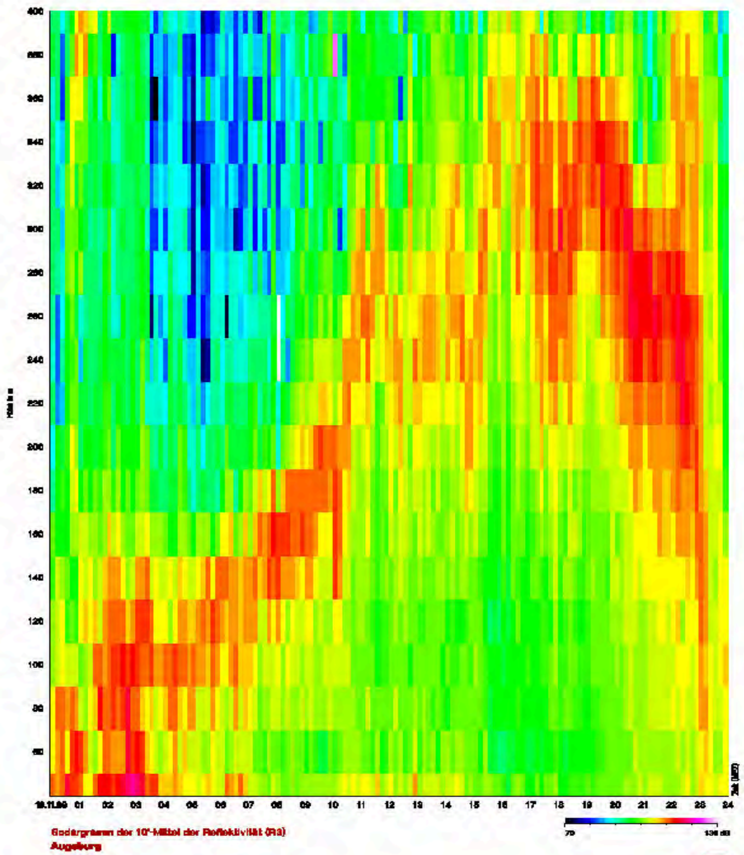

sigma w

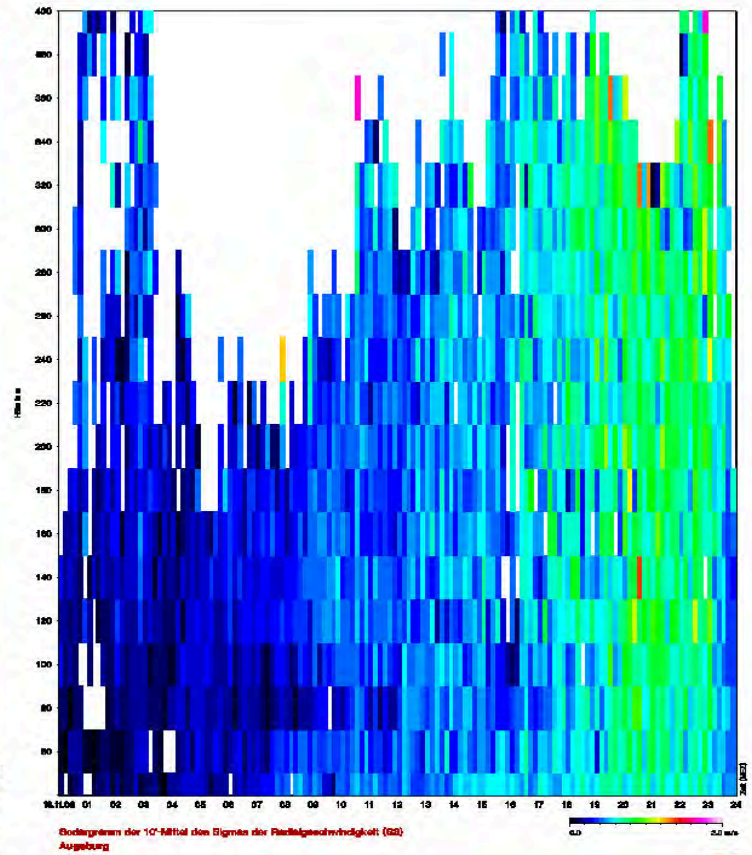

1 day, midnight to midnight

stefan.emeis@kit.edu Institute for Meteorology and Climate Research – Atmospheric Environmental Research

Algorithms to detect MLH from SODAR data

criterion 1:
upper edge of high turbulence

criterion 2:
surface and lifted inversions

MLH = Min (C1, C2)

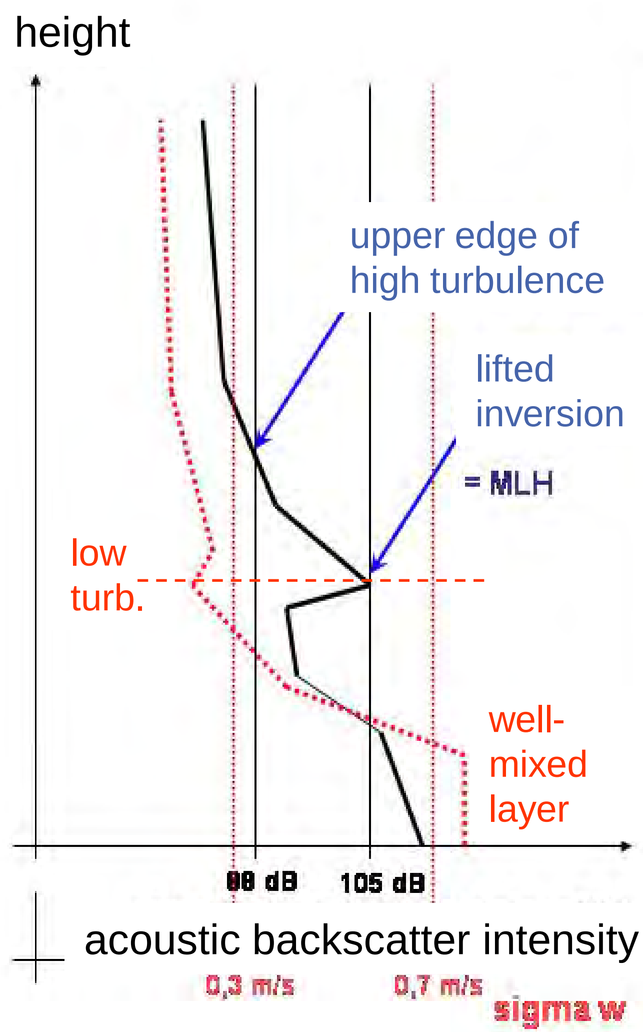

example 1: daytime

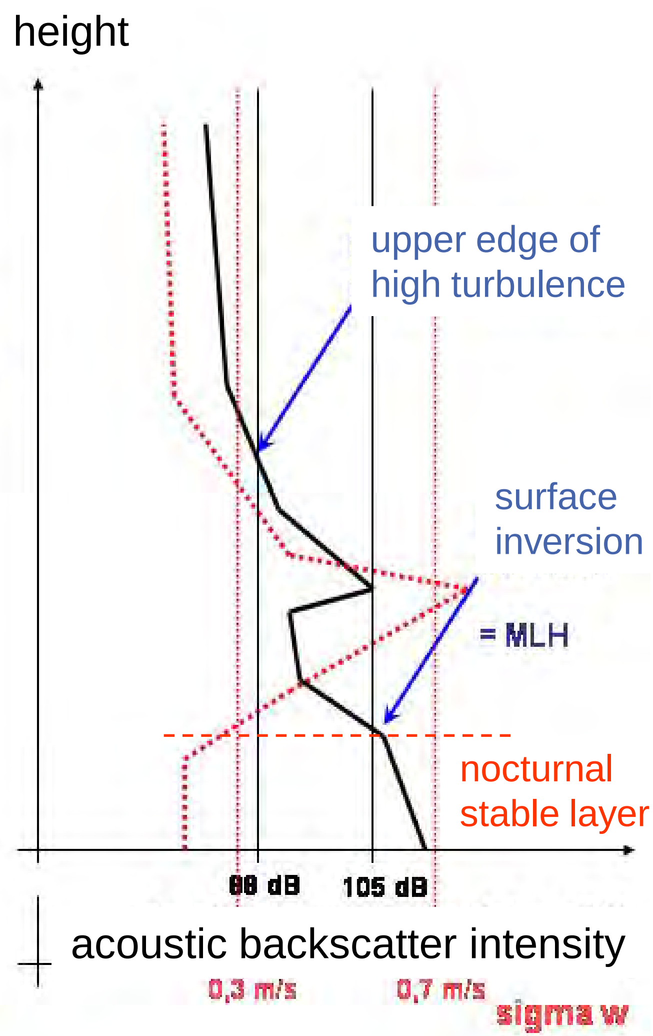

example 2: night-time

Emeis, S., K. Schäfer, C. Münkel, 2008: Surface-based remote sensing of the mixing-layer height – a review. Meteorol. Z., **17**, 621-630.

stefan.emeis@kit.edu Institute for Meteorology and Climate Research – Atmospheric Environmental Research

examples for low-level jet observations with SODAR

vertical profiles of wind speed (30 min means)

23-30 June 2005

AdP Ch d G

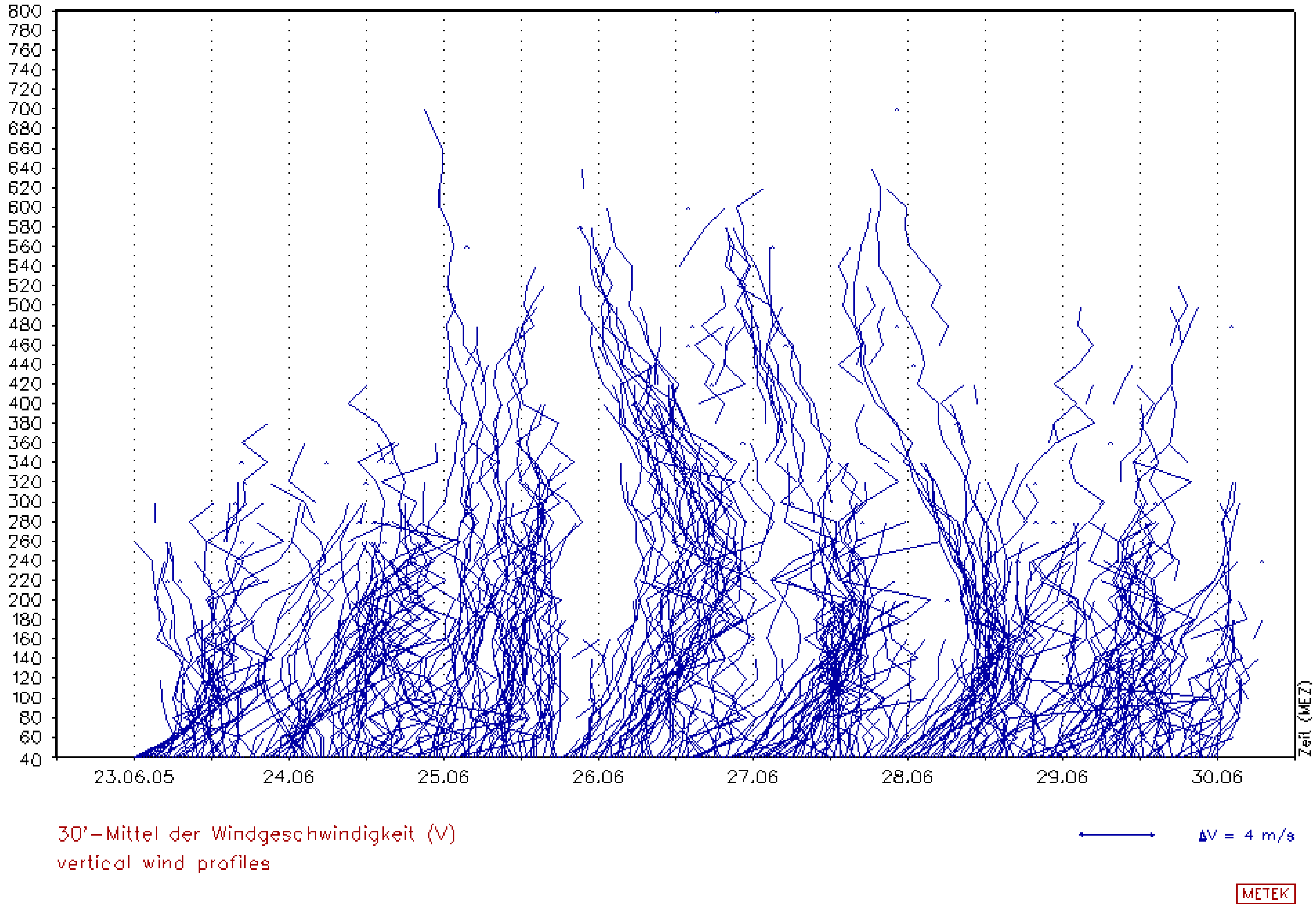

Prof. Dr. Stefan Emeis – Low-level jets stefan.emeis@kit.edu

Institute for Meteorology and Climate Research – Atmospheric Environmental Research

Monthly mean diurnal course of wind speed

August 2002, 17 nights with LLJ

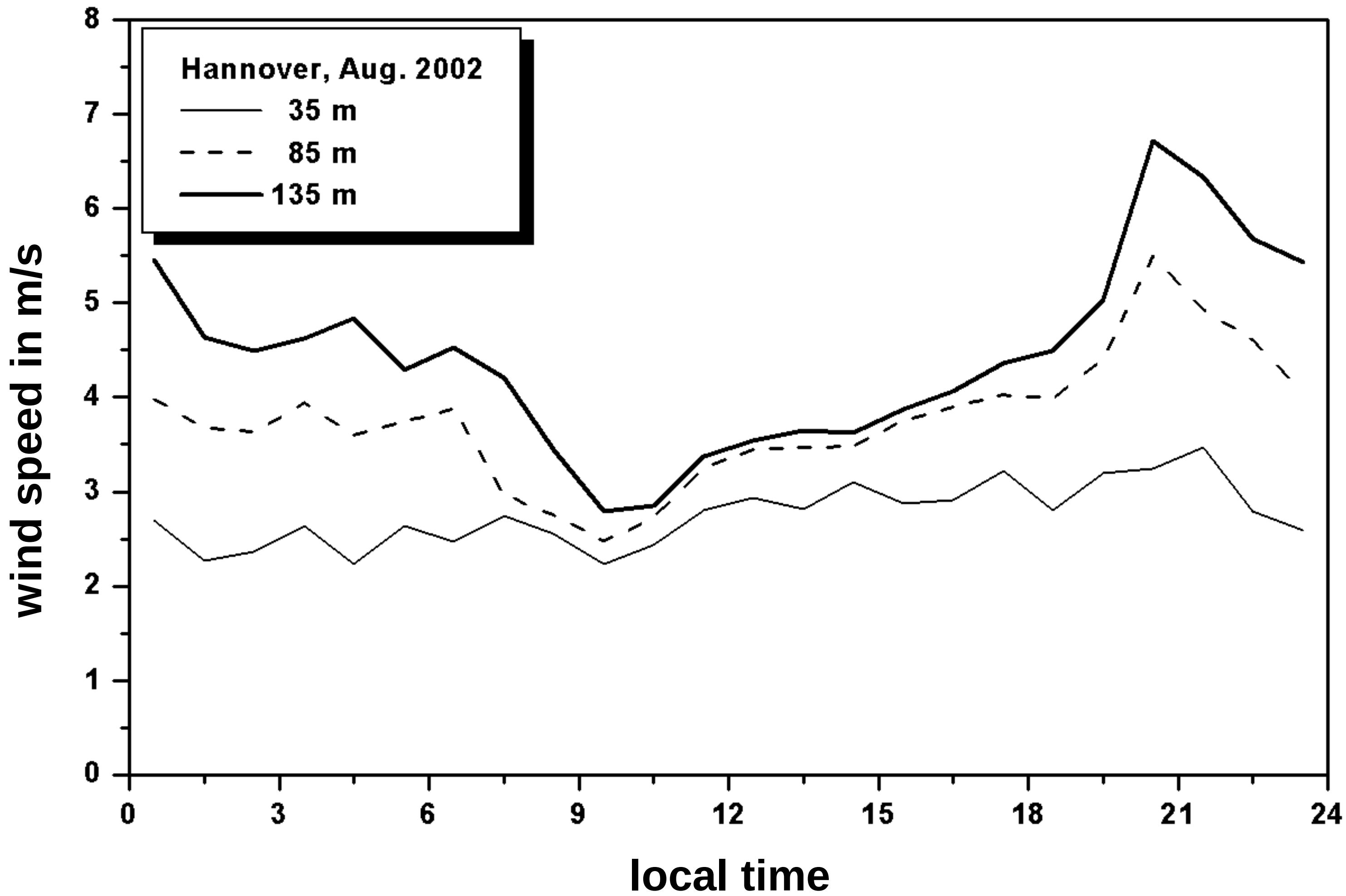

Mean diurnal variation of the turning of wind direction with height

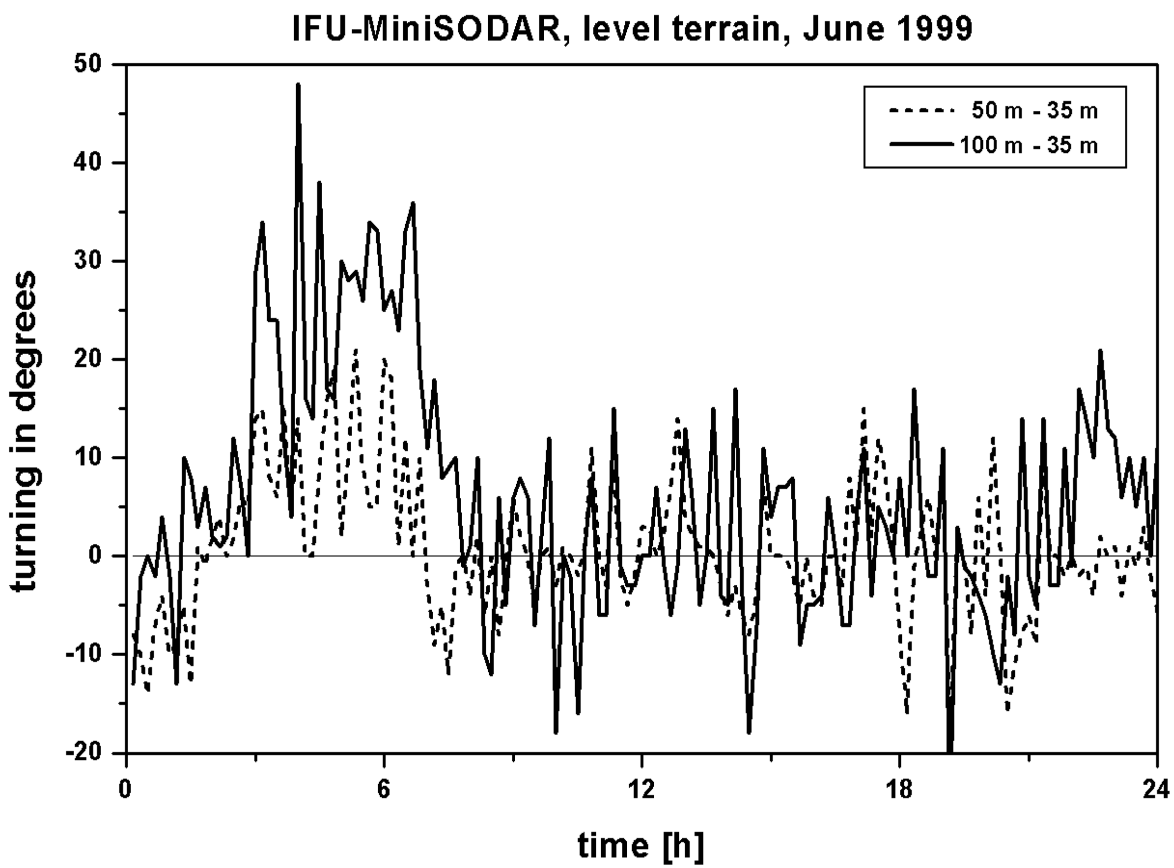

Emeis, S., 2001: Vertical variation of frequency distributions of wind speed in and above the surface layer observed by sodar. Meteorol. Z., **10**, 141-149.

Ceilometer

mixing-layer height

Ceilometer/LIDAR measuring principle

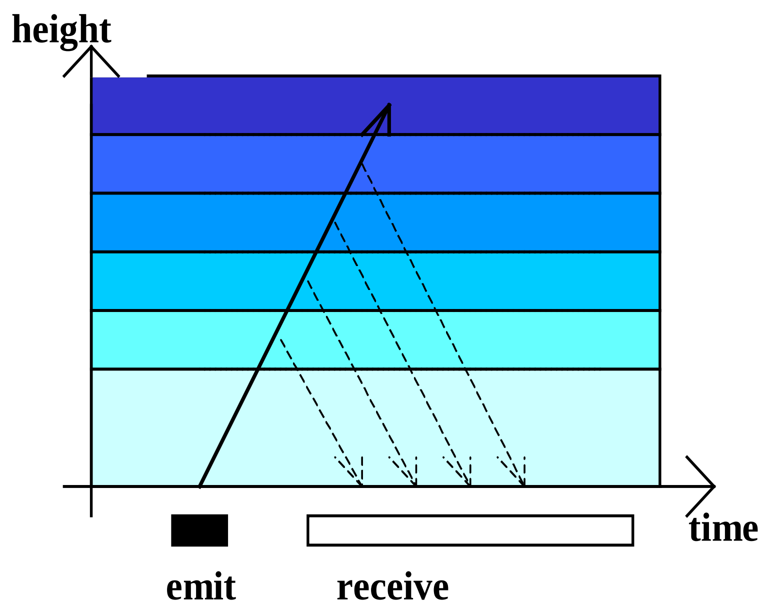

detection:

travel time of signal = height
backscatter intensity = particle size and number distribution
Doppler-shift = line-of-sight wind speed

wind-LIDAR only, cannot be analyzed from ceilometer data

WindForS Wind Energy Research Alliance

ceilometer sample plot (daytime convective BL)

Karlsruhe Institute of Technology

optical backscatter intensity

negative vertical gradient of optical backscatter intensity

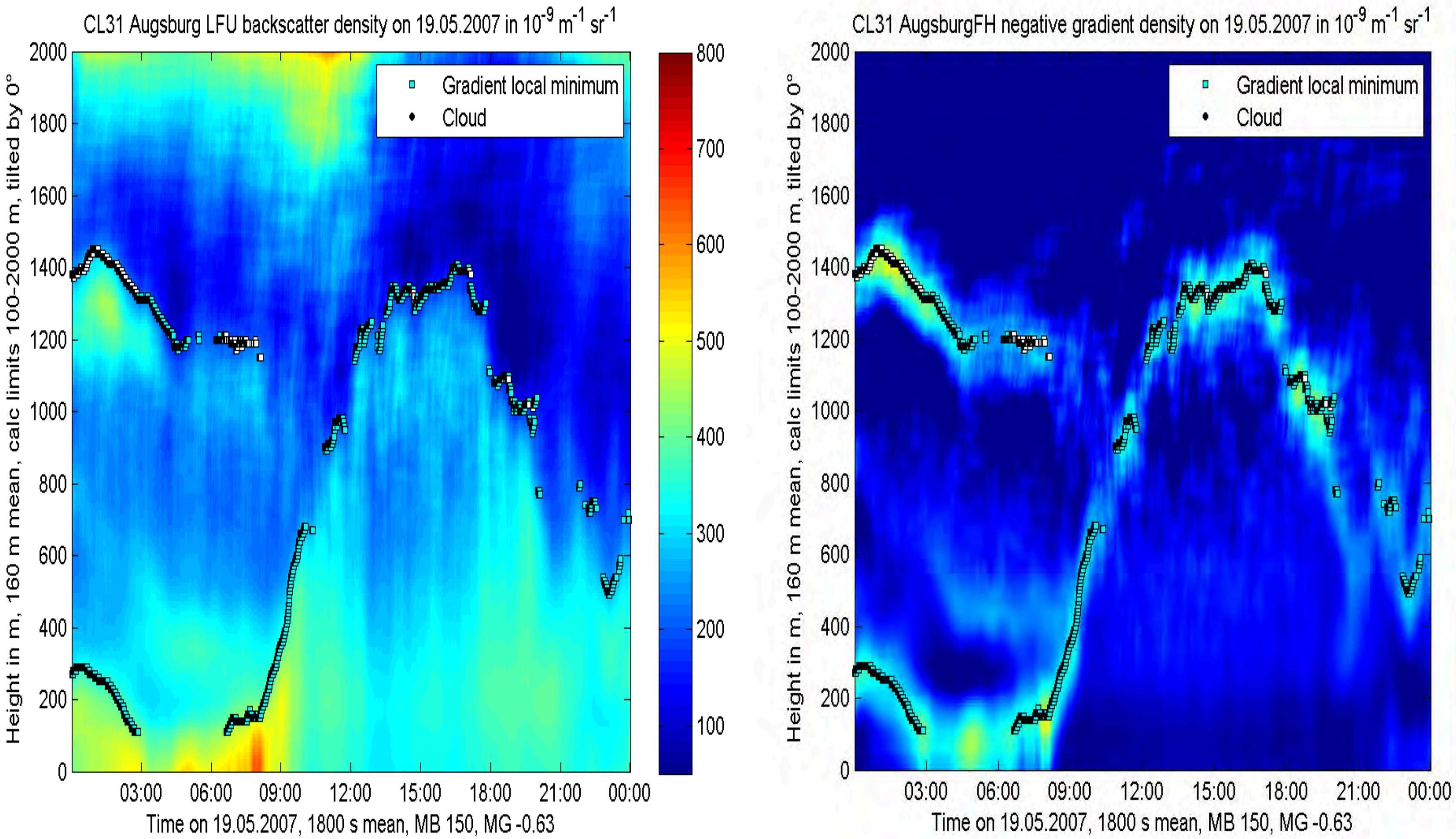

Algorithm to detect MLH from Ceilometer-Daten

criterion

minimal vertical gradient of backscatter intensity (the most negative gradient)

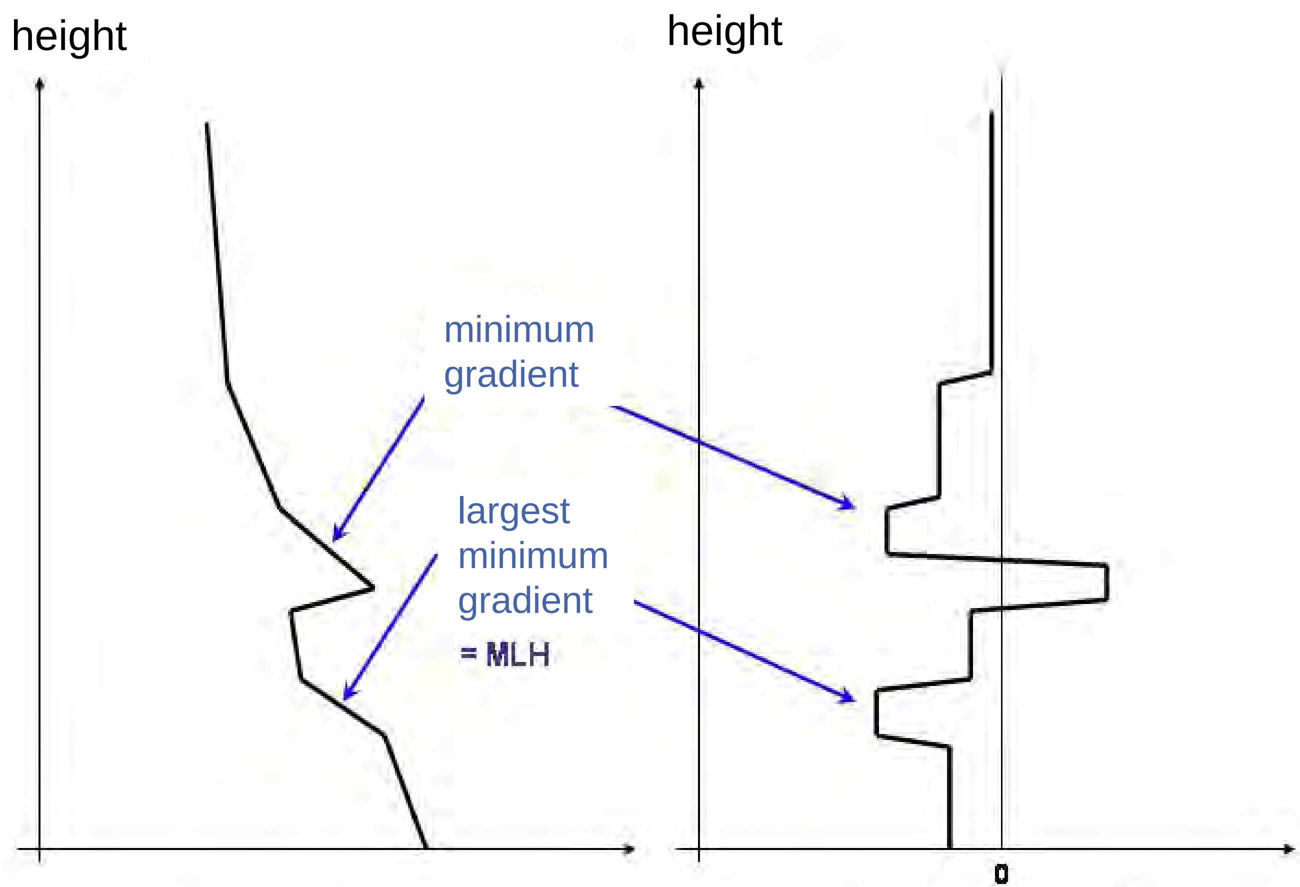

optical backscatter intensity

vertical gradient of
optical backscatter intensity

stefan.emeis@kit.edu Institute for Meteorology and Climate Research – Atmospheric Environmental Research

Different gradient methods (see Sicard et al. 2006, BLM 119, 135-157)

logarithmic gradient minimum

gradient minimum

inflection point method
(minimum of 2nd derivative)

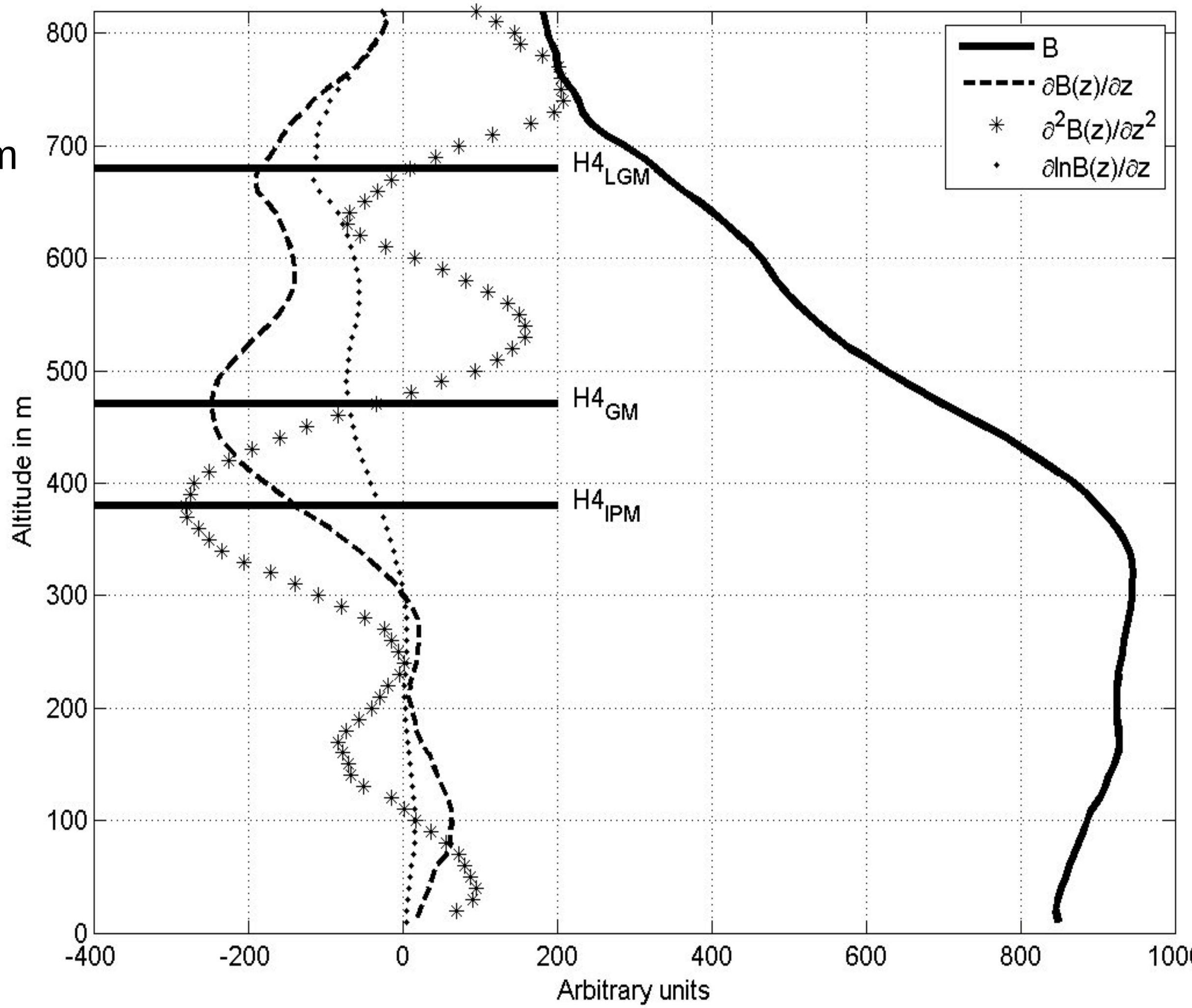

comparison of two different ceilometers

LD40

two optical axes

wave length: 855 nm

height resolution: 7.5 m

max. range: 13000 m

CL31 / CL51

one optical axis

wave length: 905 nm

height resolution: 5 m

max. range: 7500 m

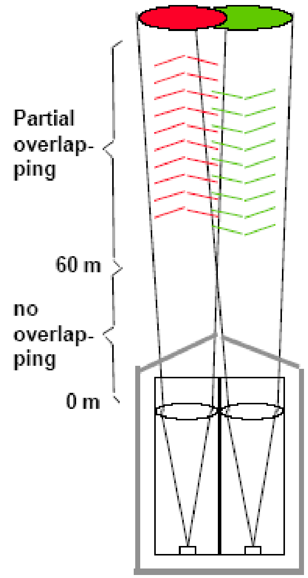

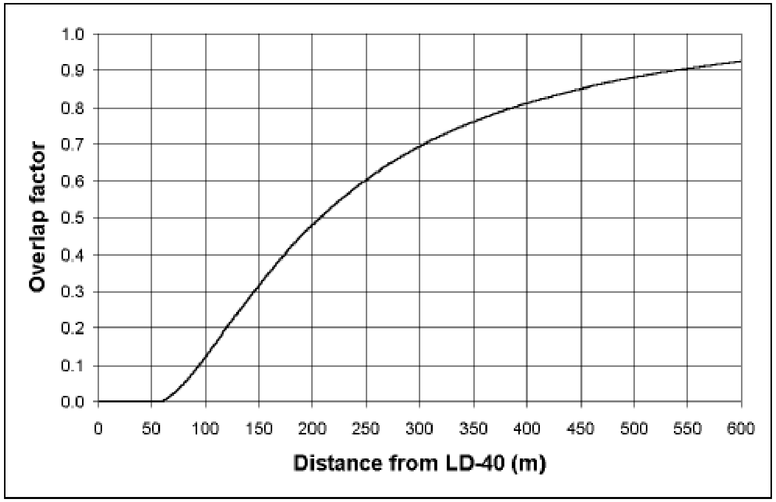

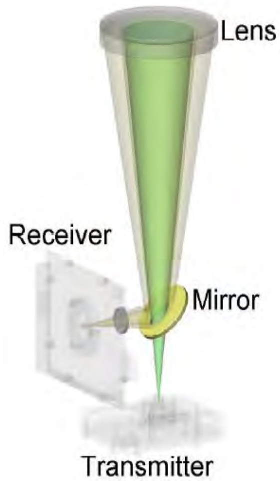

WINDFORS Wind Energy Research Alliance

comparison of LD40 and CL31

KIT Karlsruhe Institute of Technology

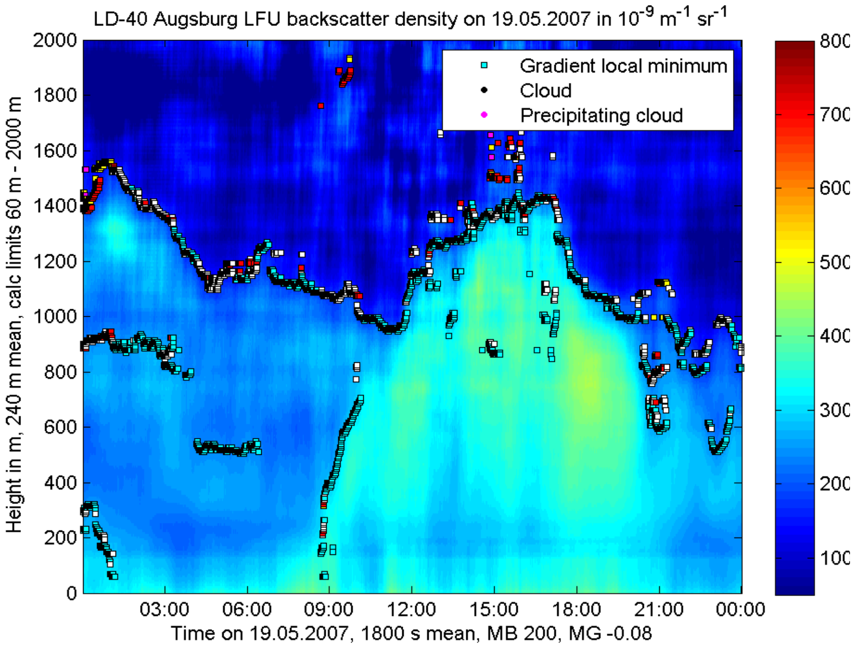

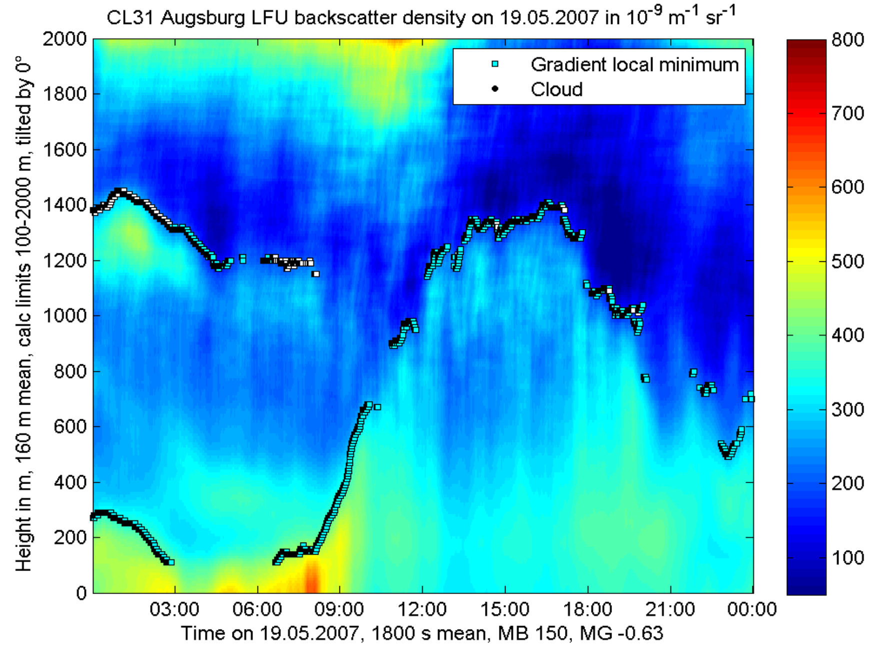

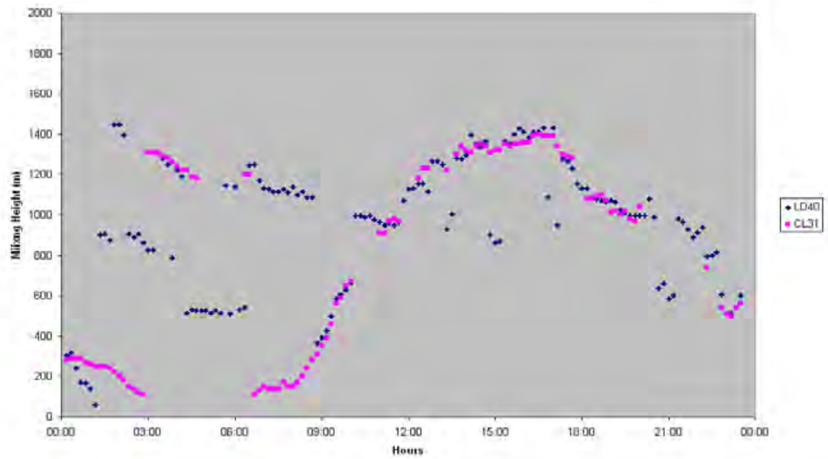

stefan.emeis@kit.edu Institute for Meteorology and Climate Research – Atmospheric Environmental Research

RASS

wind, turbulence, temperature, mixing-layer height

RASS measuring principle

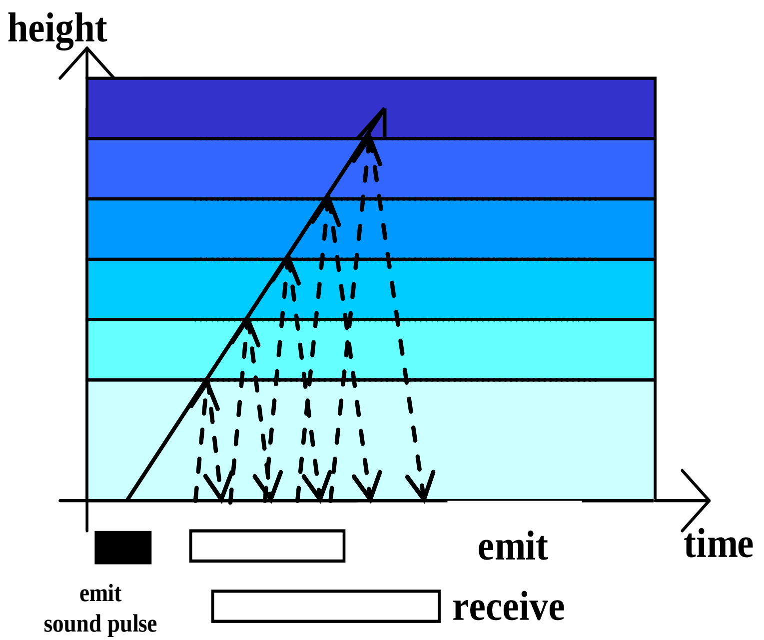

detection:

travel time of em./ac. signal = height
ac. backscatter intensity = turbulence (identical to SODAR)
ac. Doppler-shift = line-of-sight wind speed (identical to SODAR)
em. Doppler shift = sound speed ➔ temperature

RASS: frequencies

Bragg condition:
acoustic wavelength = ½ electro-magnetic wavelength

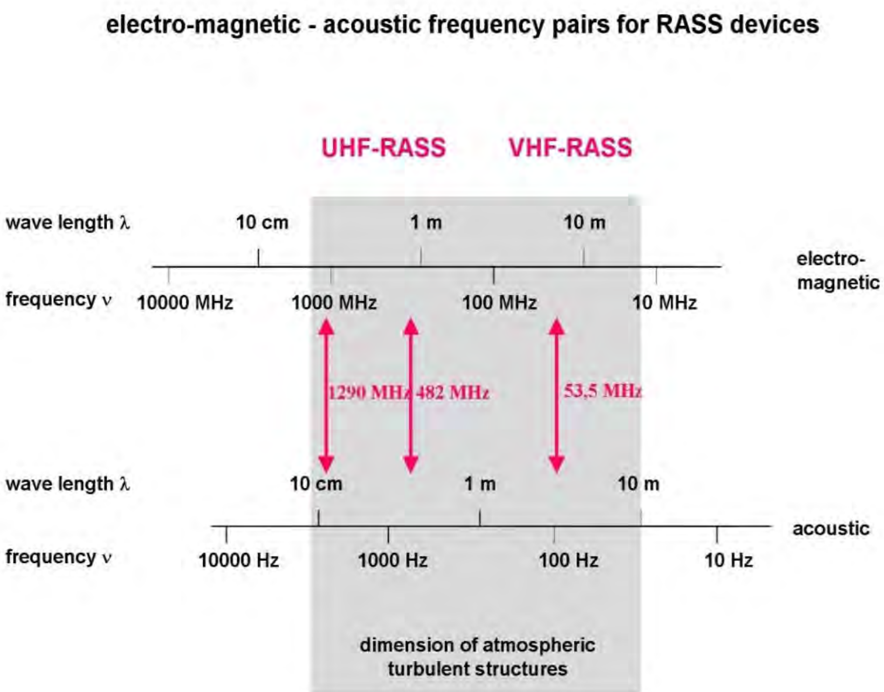

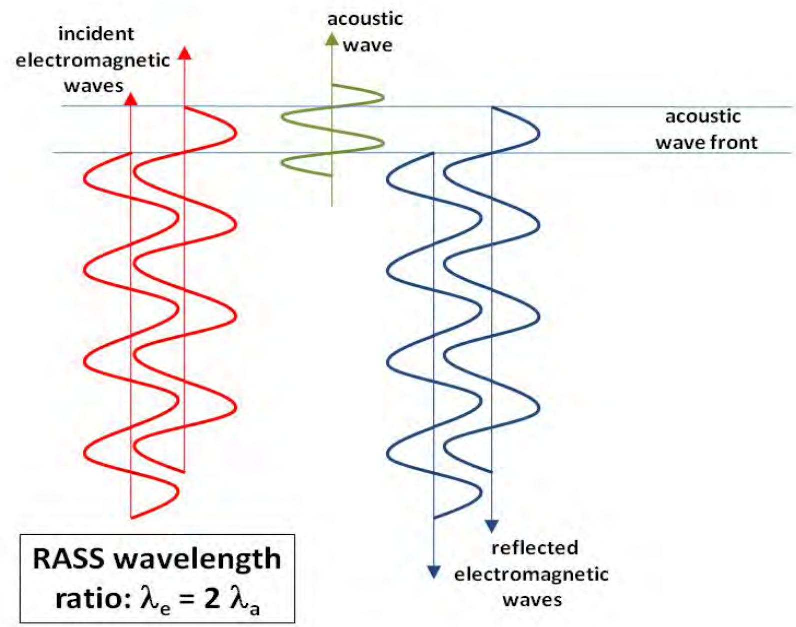

Emeis, S., 2010: Measurement Methods in Atmospheric Sciences - In situ and remote. Borntraeger, Stuttgart, 272 pp., 103 figs, 28 tables, ISBN 978-3-443-01066-9.

SODAR-RASS
(Doppler-RASS)

(METEK)

acoustic frequ.: 1077 Hz
radio frequ.: 474 MHz
resolution: 20 m
lowest
range gate: ca. 40 m

vertical range: 540 m

example RASS data: summer day
potential temperature (left), horizontal wind (right)

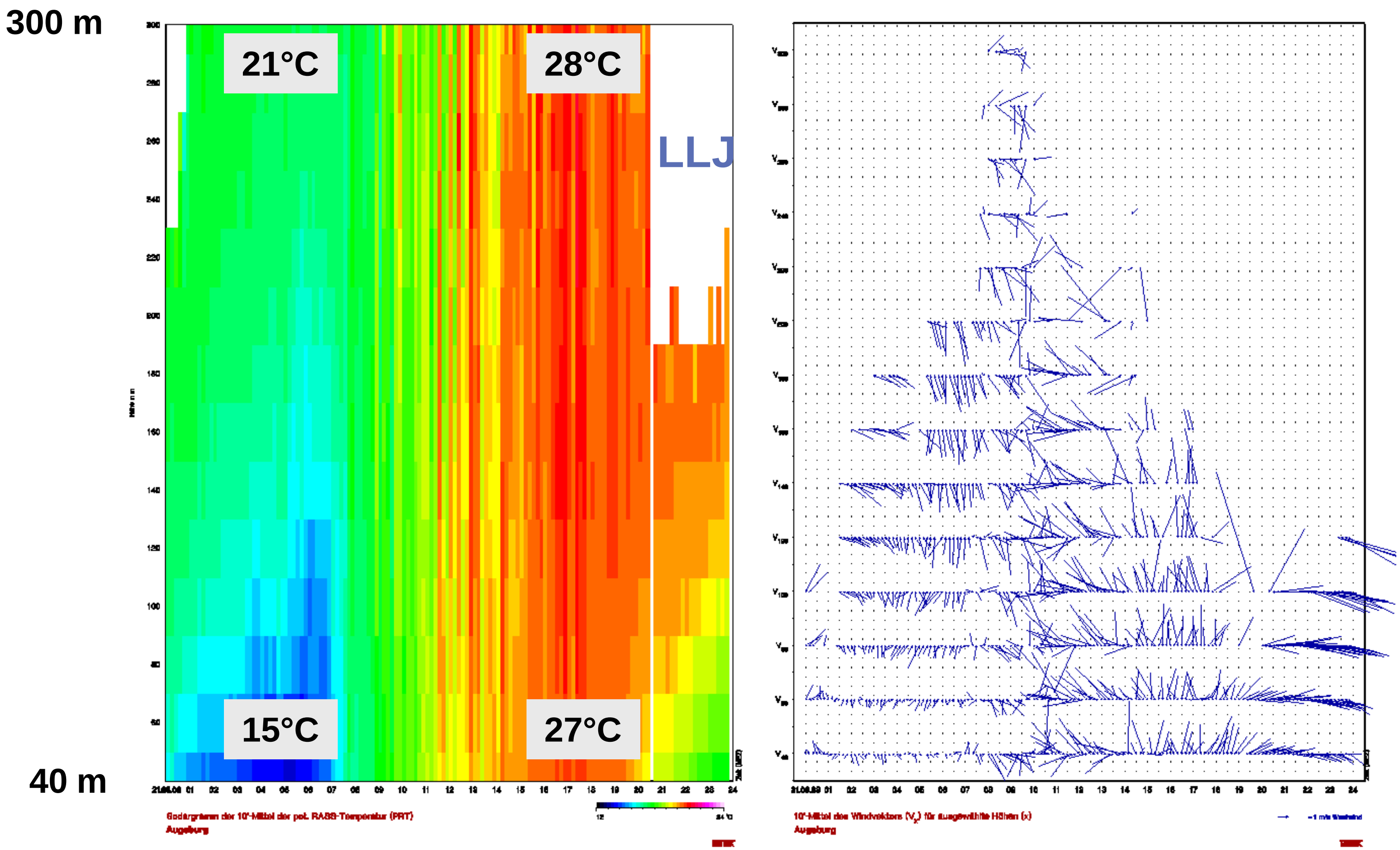

example RASS data: winter day
potential temperature (left), horizontal wind (right)

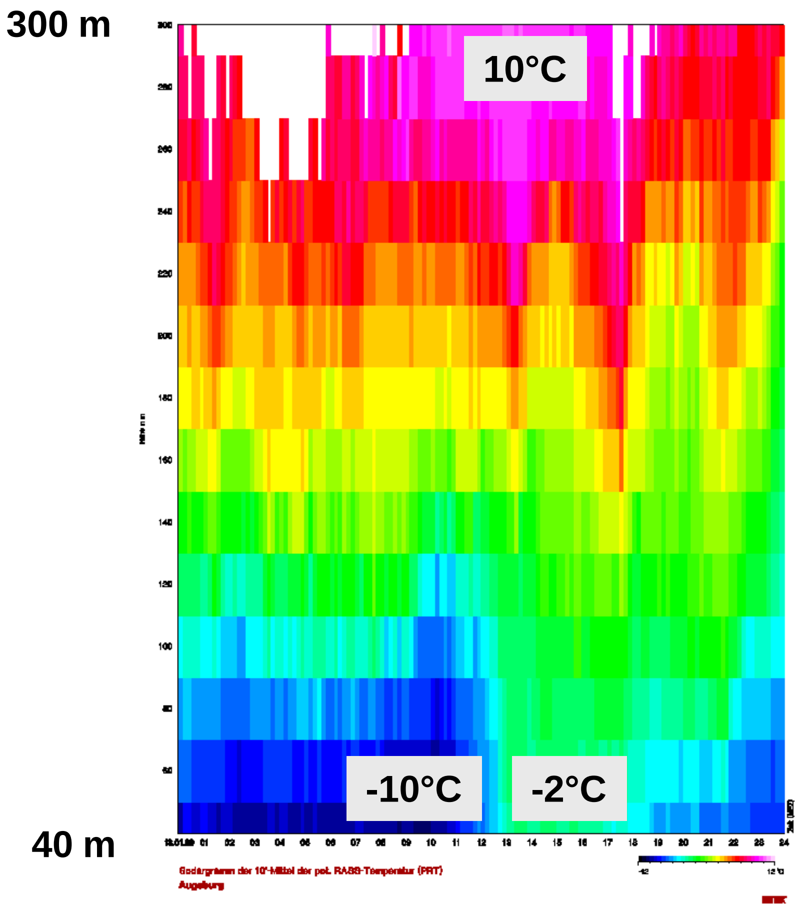

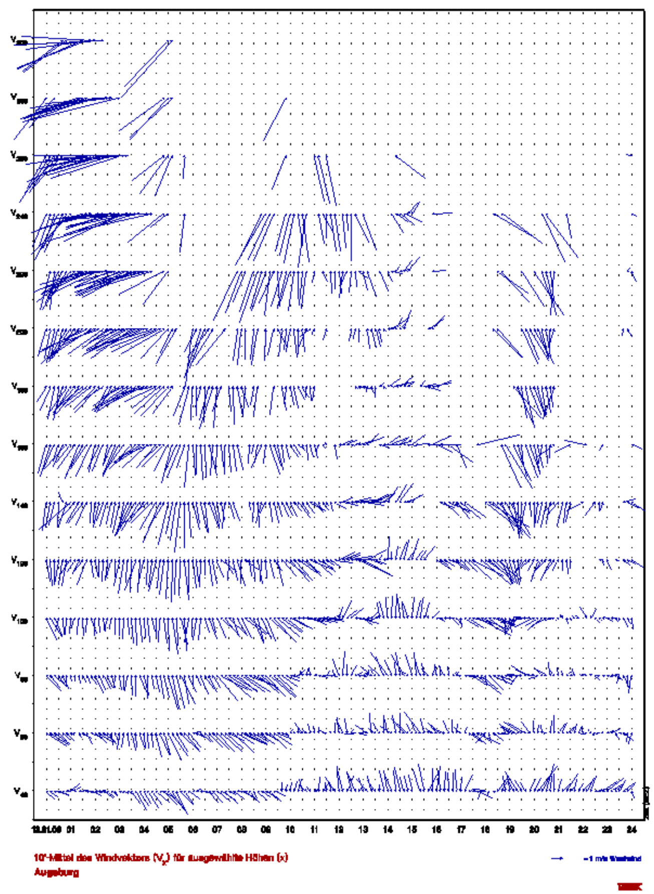

WindForS Wind Energy Research Alliance

KIT Karlsruhe Institute of Technology

example RASS data: inversion potential temperature (left), horizontal wind (right)

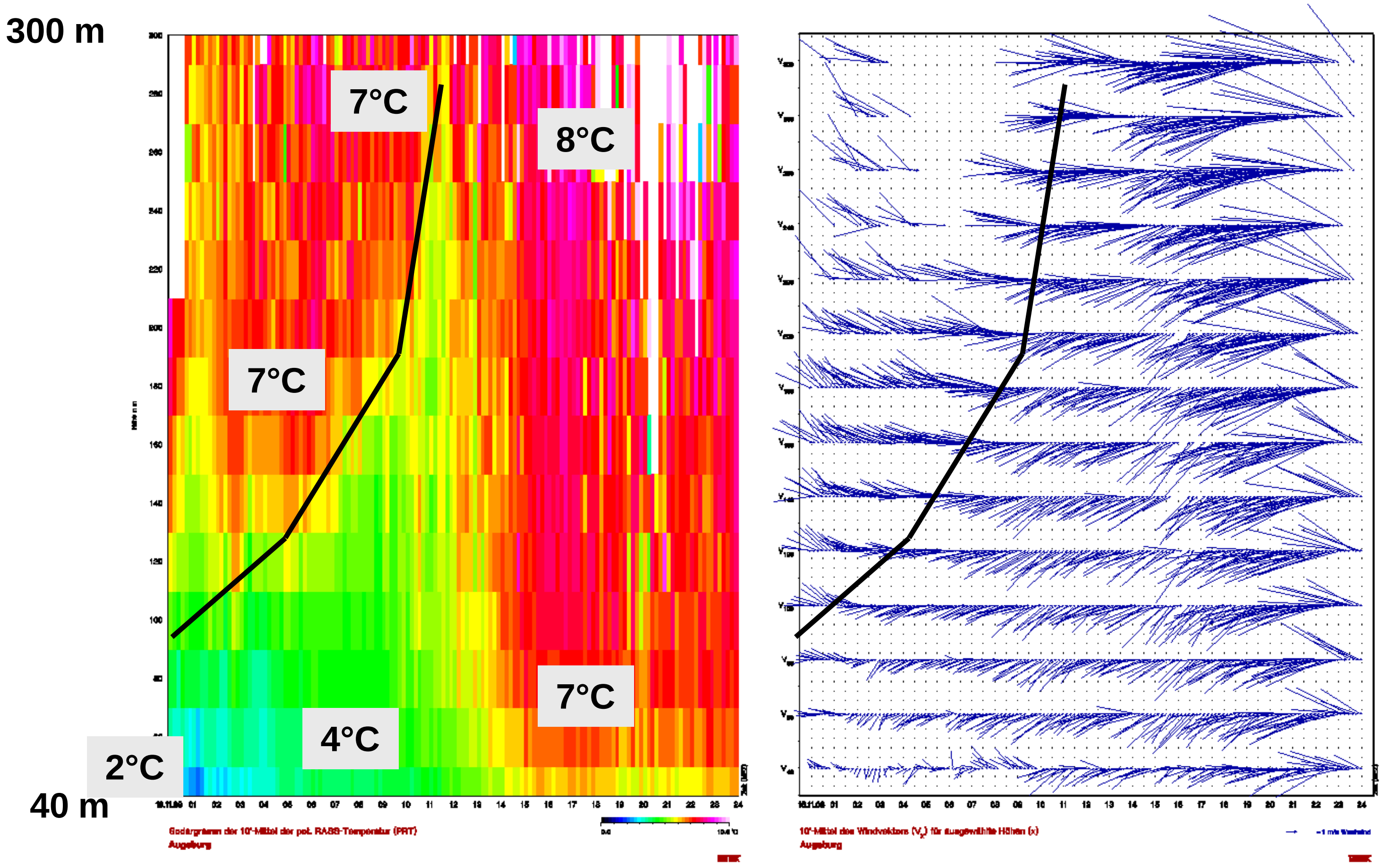

stefan.emeis@kit.edu Institute for Meteorology and Climate Research – Atmospheric Environmental Research

RASS (radio-acoustic remote sensing)

Bragg-RASS: windprofiler plus acoustic component

Doppler-RASS: SODAR plus electro-magnetic component

UHF RASS (boundary layer)

VHF RASS (troposphere)

stefan.emeis@kit.edu Institute for Meteorology and Climate Research – Atmospheric Environmental Research

Doppler windlidar

wind, turbulence, mixing-layer height, low-level jet

stefan.emeis@kit.edu Institute for Meteorology and Climate Research – Atmospheric Environmental Research

Doppler windlidar measuring principle

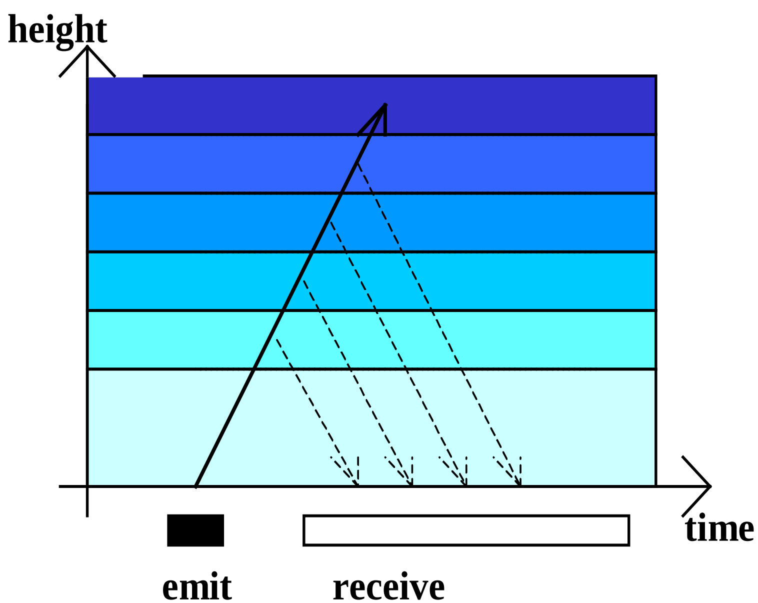

detection:

travel time of signal = height
backscatter intensity = particle size and number distribution
depolarisation = particle shape
Doppler-shift = wind speed in the line of sight

stefan.emeis@kit.edu Institute for Meteorology and Climate Research – Atmospheric Environmental Research

mobile Doppler windlidar from Halo Photonics

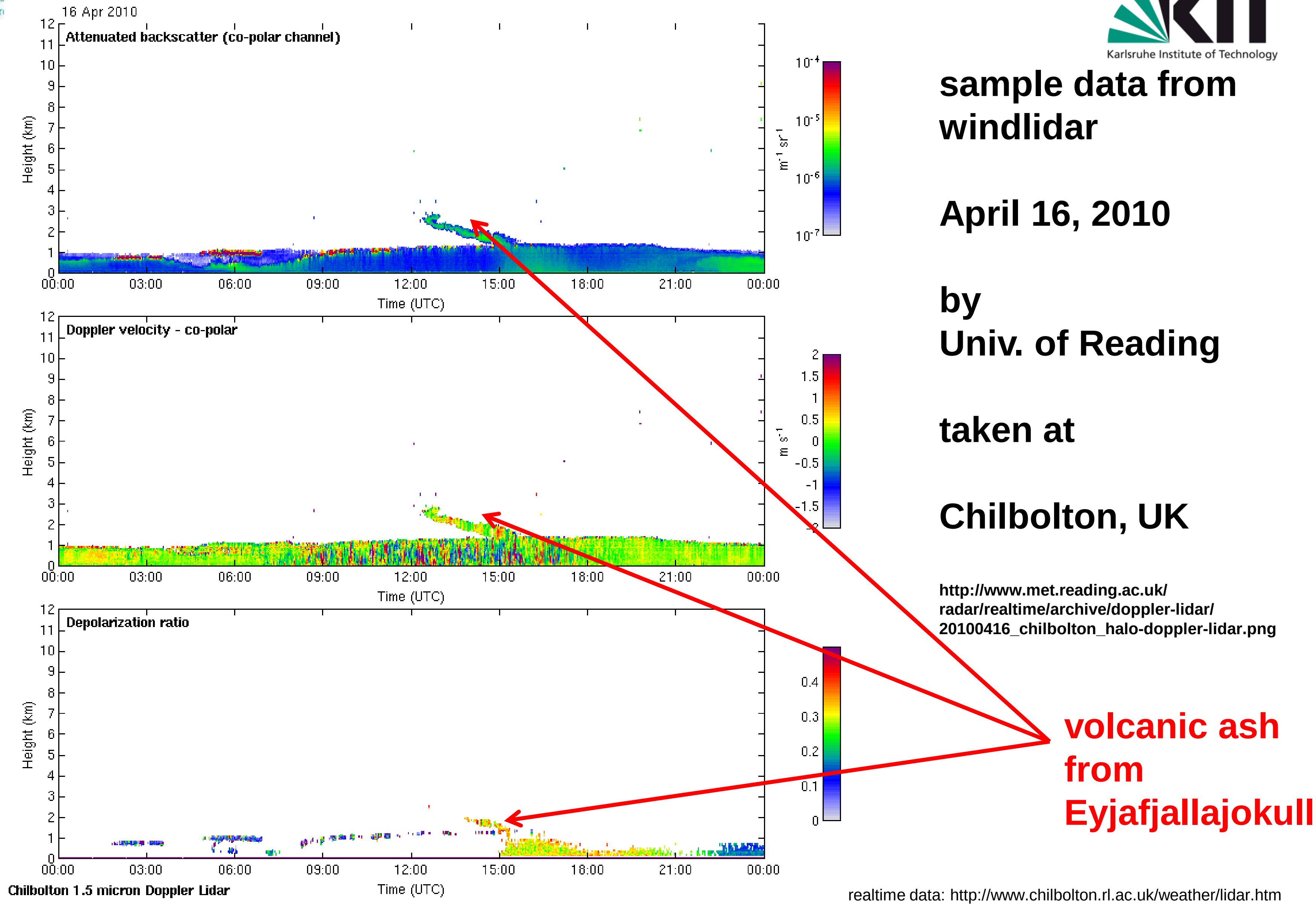

sample data from windlidar

April 16, 2010

by Univ. of Reading

taken at

Chilbolton, UK

http://www.met.reading.ac.uk/radar/realtime/archive/doppler-lidar/20100416_chilbolton_halo-doppler-lidar.png

realtime data: http://www.chilbolton.rl.ac.uk/weather/lidar.htm

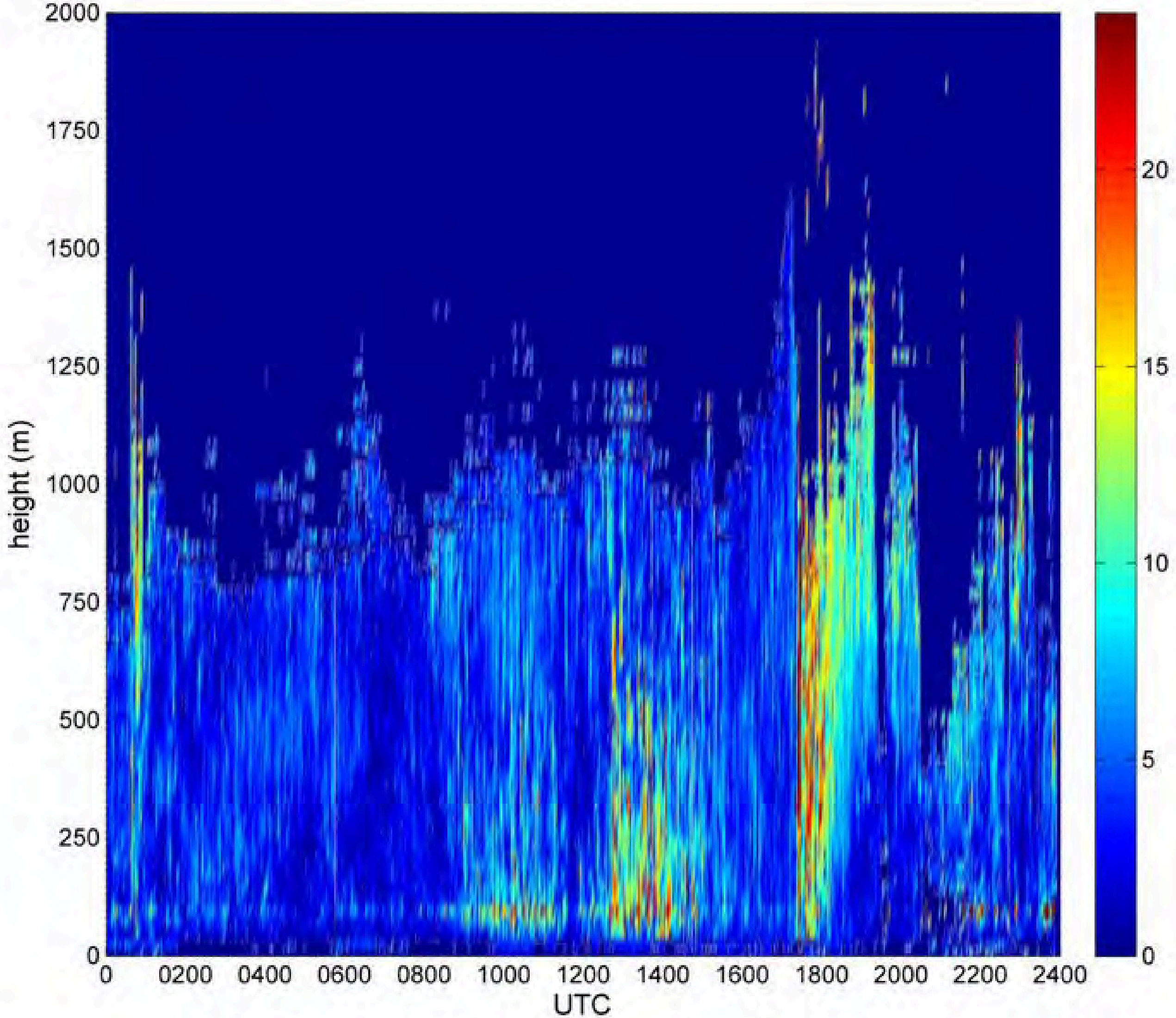

sample data from windlidar

wind speeds in m/s (colour bar)

June 22, 2011

by IMK-IFU

taken at

Garmisch-Partenk., Germany

Comparisons between different instruments

temperature profile and aerosol backscatter

comparison of RASS data (potential temperature, right) with aerosol backscatter from a ceilometer (left)

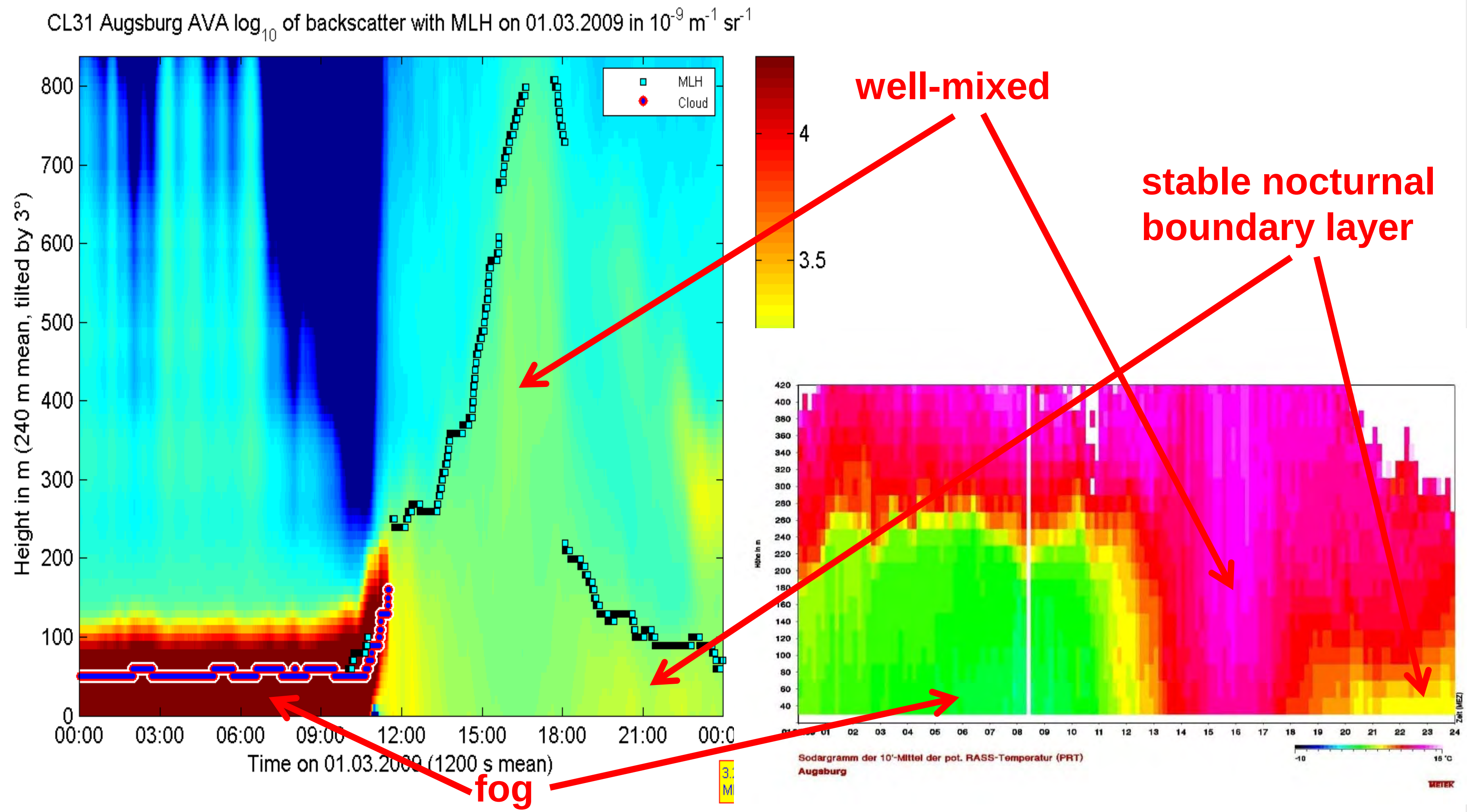

stefan.emeis@kit.edu Institute for Meteorology and Climate Research – Atmospheric Environmental Research

Detection of the diurnal variation of PBL structure from SODAR and Ceilometer data taken in Budapest

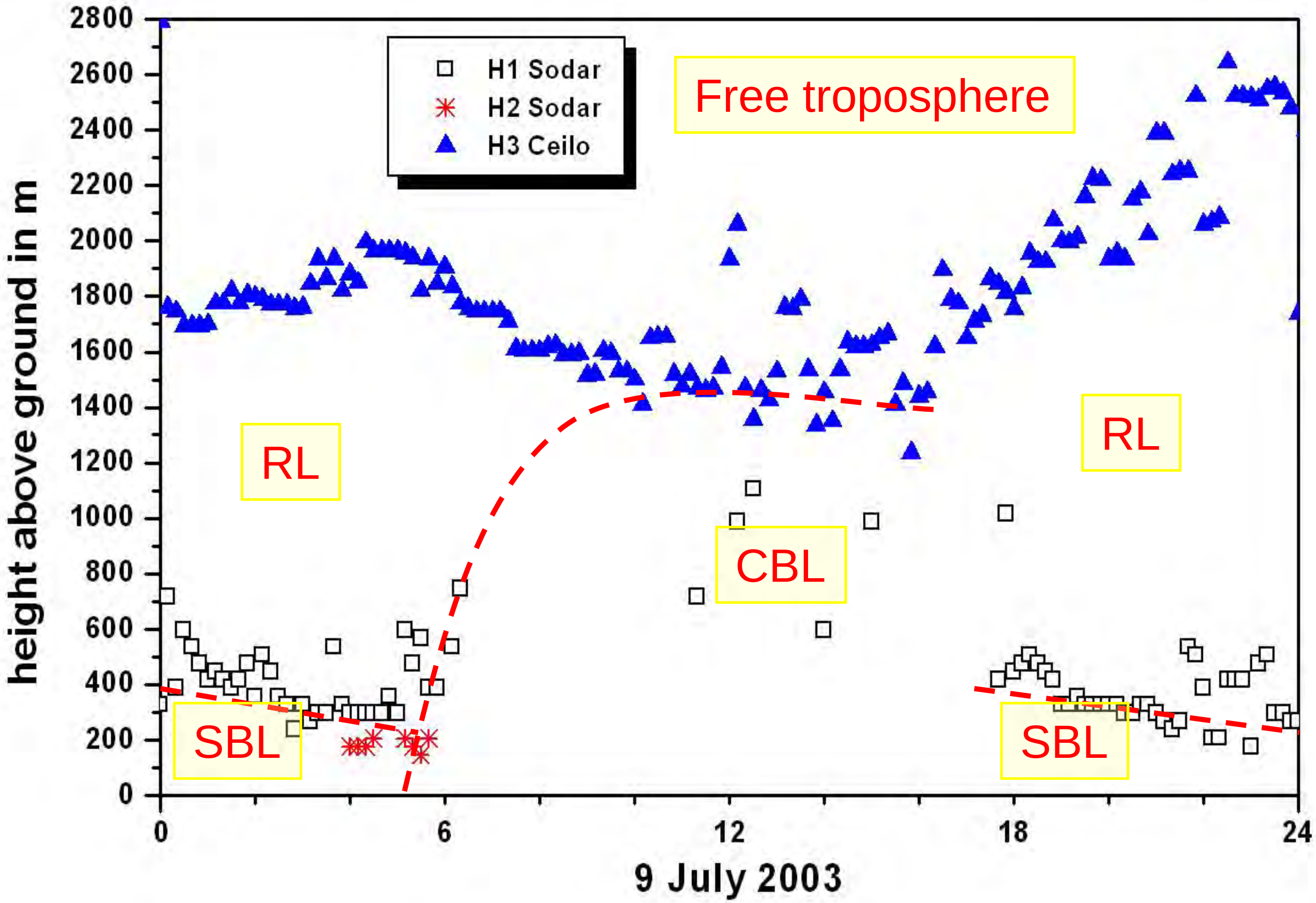

SBL:

stable boundary layer (usually at night and in winter)

CBL:

convective boundary layer (usually at daytime due to strong insolation)

RL:

residual layer (usually at nighttime)

Emeis, S., K. Schäfer, 2006: Remote sensing methods to investigate boundary-layer structures relevant to air pollution in cities. Bound.-Lay Meteorol., 121, 377-385,

Differences in MLH detection from SODAR and Ceilometer data taken in Budapest

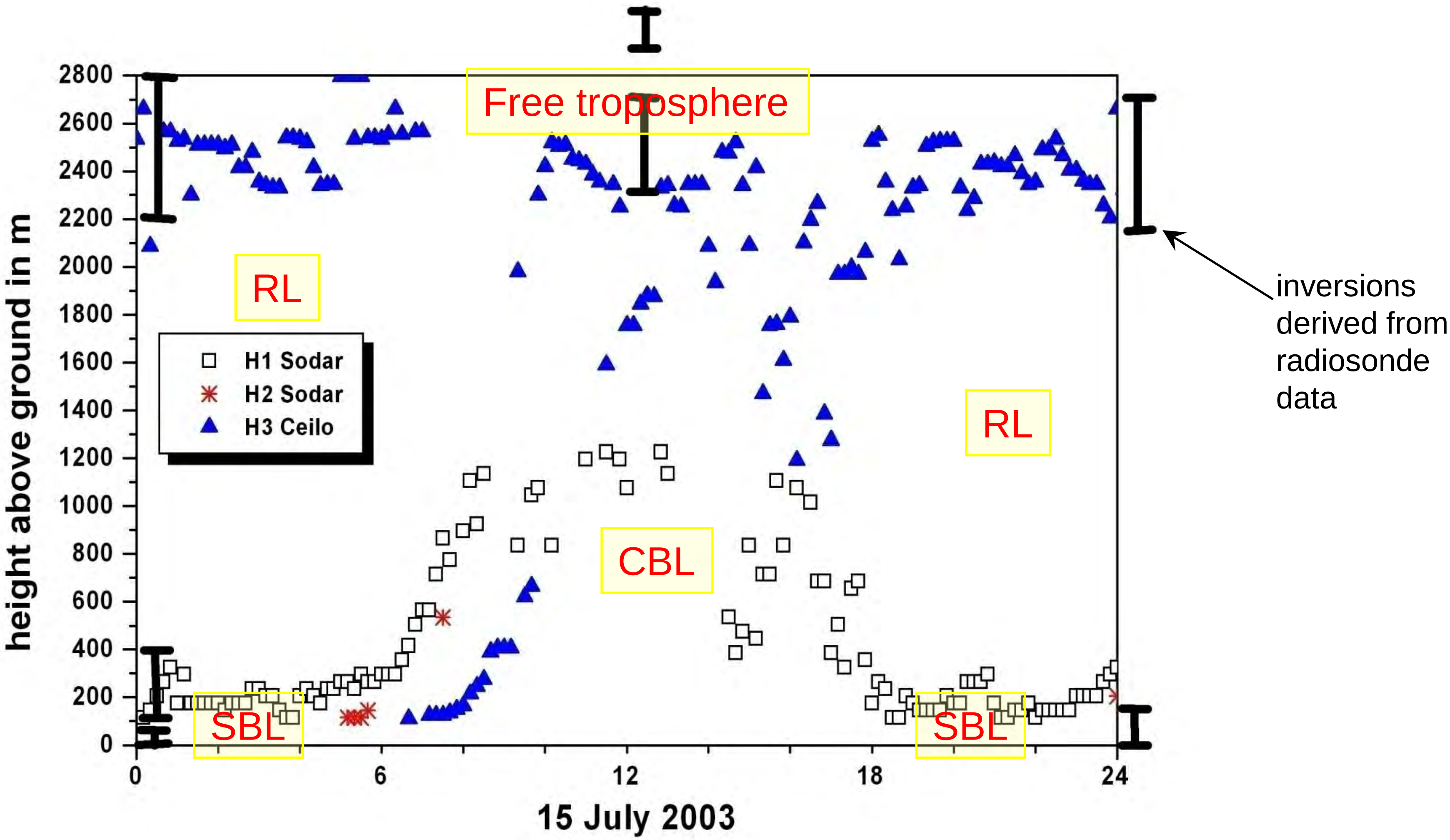

Emeis, S., K. Schäfer, 2006: Remote sensing methods to investigate boundary-layer structures relevant to air pollution in cities. Bound.-Lay Meteorol., 121, 377-385,

RASS data Augsburg February 2009

potential temperature (top), backscatter SODAR (middle), Ceilometer (bottom)

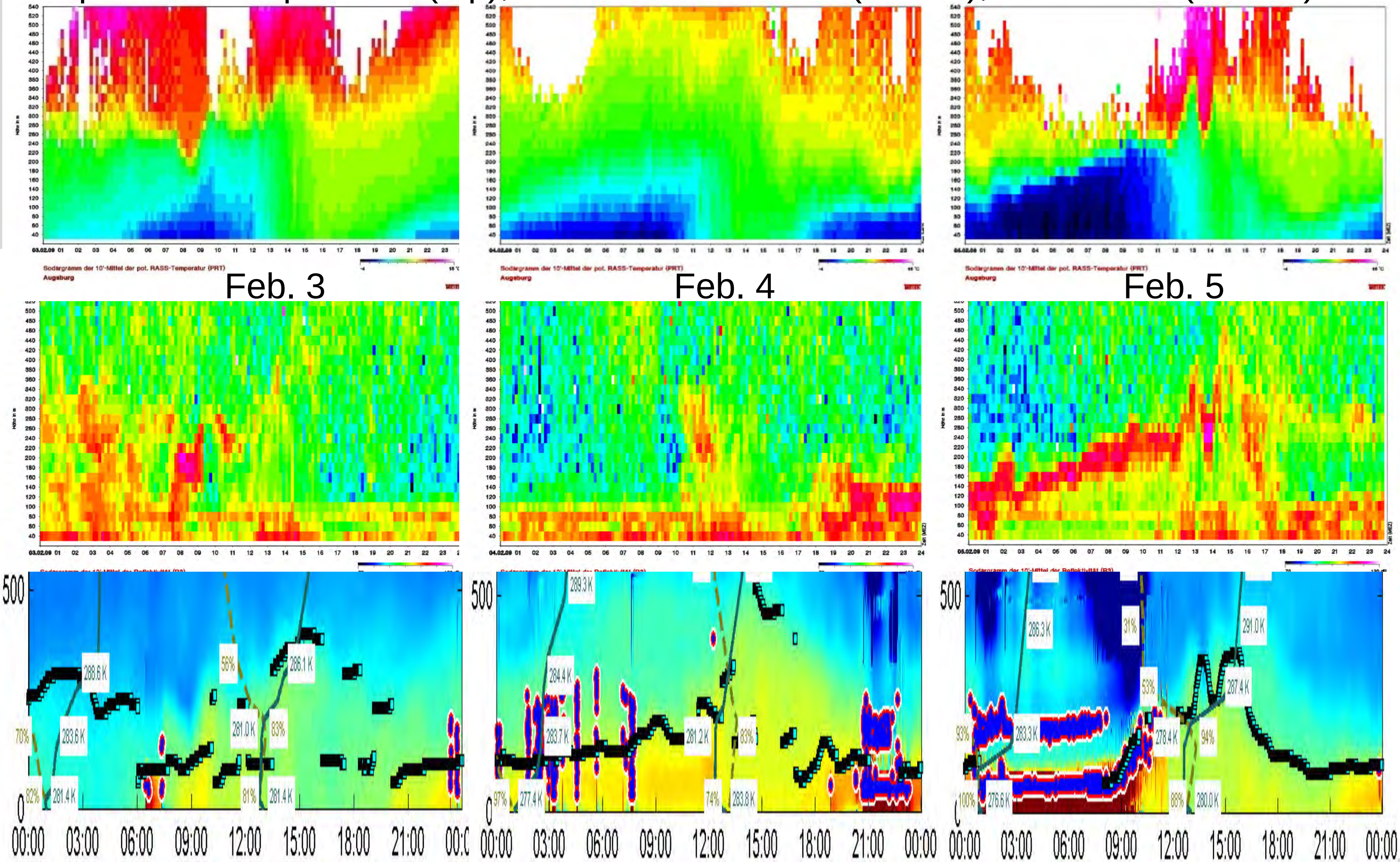

stefan.emeis@kit.edu Institute for Meteorology and Climate Research – Atmospheric Environmental Research

Summary

stefan.emeis@kit.edu Institute for Meteorology and Climate Research – Atmospheric Environmental Research

☺ ☺ ☺ 💣 **RASS** **delivers temperature profiles, wind profiles are additionally available.**
MLH directly from temperature profiles. LLJ from wind profiles.
Does not work properly under high wind speeds. Restricted range.

☺ ☺ ☺ 💣 **wind lidar** **detects wind profiles, aerosol distribution and water droplets. It has to be assumed that the aerosol follows the thermal structure of the atmosphere and the wind.**
MLH from aerosol backscatter, wind speed variance, LLJ from wind profiles.
Does not work properly in extreme clear (aerosol-free) air and during precipitation events and fog.

☺ ☺ 💣 💣 **Ceilometer** **detects aerosol distribution and water droplets. It has to be assumed that the aerosol follows the thermal structure of the atmosphere.**
MLH indirectly from aerosol backscatter using a MLH algorithm.
Does not work properly in extreme clear (aerosol-free) air and during precipitation events and fog.

☺ 💣 💣 💣 **SODAR** **detects wind profiles, temperature fluctuations and gradients, but no absolute temperature.**
MLH indirectly from acoustic backscatter (MLH algorithm). LLJ from wind profiles.
Does not work properly under perfectly neutral stratification, with very high wind speeds, and during stronger precipitation events. Restricted range.

Literature

SODAR:

Asimakopoulos, D.N., C.G. Helmis, J. Michopoulos, 2004: Evaluation of SODAR methods for the determination of the atmospheric boundary layer mixing height. - Meteor. Atmos. Phys. 85, 85–92.

Beyrich, F., 1997: Mixing height estimation from sodar data – a critical discussion. - Atmos. Environ. 31, 3941–3953.

Ceilometer:

Schäfer, K., S.M. Emeis, A. Rauch, C. Münkel, S. Vogt, 2004: Determination of mixing-layer heights from ceilometer data. In: Remote Sensing of Clouds and the Atmosphere IX. Schäfer, K., A. Comeron, M. Carleer, R.H. Picard, N. Sifakis (Eds.), Proc. SPIE, Bellingham, WA, USA, Vol. 5571, 248–259.

Sicard, M., C. Pérez, F. Rocadenbosch, J.M. Baldasano, D. García-Vizcaino, 2006: Mixed-Layer Depth Determination in the Barcelona Coastal Area From Regular Lidar Measurements: Methods, Results and Limitations. - Bound.-Lay. Meteor. 119, 135–157.

RASS:

Engelbart, D.A.M., J. Bange, 2002: Determination of boundary-layer parameters using wind profiler/RASS and sodar/RASS in the frame of the LITFASS project. Theor. Appl. Climatol. 73, 53–65.

Emeis, S., K. Schäfer, C. Münkel, 2009: Observation of the structure of the urban boundary layer with different ceilometers and validation by RASS data. Meteorol. Z., 18, 149-154. (Open access, freely available from http://dx.doi.org/10.1127/0941-2948/2009/0365)

Emeis, S., K. Schäfer, C. Münkel, R. Friedl, P. Suppan, 2011: Evaluation of the interpretation of ceilometer data with RASS and radiosonde data. Bound.-Lay. Meteorol., online April 5, 2011. DOI: 10.1007/s10546-011-9604-6

Windlidar:

Emeis, S., M. Harris, R.M. Banta, 2007: Boundary-layer anemometry by optical remote sensing for wind energy applications. - Meteorol. Z., 16, 337-347.

Reviews:

Emeis, S., K. Schäfer, C. Münkel, 2008: Surface-based remote sensing of the mixing-layer height – a review. - Meteorol. Z., 17, 621-630. (Open access, freely available from http://dx.doi.org/10.1127/0941-2948/2008/0312)

Books:

Wind energy meteorology

Emeis, S., 2012: Wind Energy Meteorology - Atmospheric physics for wind power generation. Springer Heidelberg etc., to appear in August 2012. ISBN: ISBN 978-3-642-30522-1

boundary-layer remote sensing with application examples:

Emeis, S., 2011: Surface-Based Remote Sensing of the Atmospheric Boundary Layer. Series: Atmospheric and Oceanographic Sciences Library, Vol. 40. Springer Heidelberg etc., X+174 pp. 114 illus., 57 in color., H/C. ISBN: 978-90-481-9339-4, DOI: 10.1007/978-90-481-9340-0

overview on the entire range of meteorological measurement methods:

Emeis, S., 2010: Measurement Methods in Atmospheric Sciences. In situ and remote. Series: Quantifying the Environment Vol. 1. Borntraeger Stuttgart. XIV+257 pp., 103 Figs, 28 Tab. ISBN 978-3-443-01066-9.

stefan.emeis@kit.edu Institute for Meteorology and Climate Research – Atmospheric Environmental Research

Thank you very much for your attention